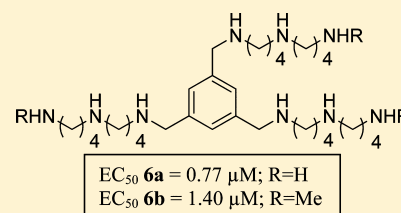


Polyamine Transport Inhibitors: Design, Synthesis, and Combination Therapies with Difluoromethylornithine

Aaron Muth,[†] Meenu Madan,[‡] Jennifer Julian Archer,[‡] Nicolette Ocampo,[†] Luis Rodriguez,[†] and Otto Phanstiel, IV^{*,‡}[†]Department of Chemistry, University of Central Florida, 4000 Central Florida Boulevard, Orlando, Florida 32816-2366, United States[‡]Department of Medical Education, 12722 Research Parkway, University of Central Florida, Orlando, Florida 32826-3227, United States

S Supporting Information

ABSTRACT: The development of polyamine transport inhibitors (PTIs), in combination with the polyamine biosynthesis inhibitor difluoromethylornithine (DFMO), provides a method to target cancers with high polyamine requirements. The DFMO+PTI combination therapy results in sustained intracellular polyamine depletion and cell death. A series of substituted benzene derivatives were evaluated for their ability to inhibit the import of spermidine in DFMO-treated Chinese hamster ovary (CHO) and L3.6pl human pancreatic cancer cells. Several design features were discovered which strongly influenced PTI potency, sensitivity to amine oxidases, and cytotoxicity. These included changes in (a) the number of polyamine chains appended to the ring system, (b) the polyamine sequence, (c) the attachment linkage of the polyamine to the aryl core, and (d) the presence of a terminal *N*-methyl group. Of the series tested, the optimal design was *N*¹,*N*^{1'},*N*^{1''}-(benzene-1,3,5-triyltris(methylene))tris(*N*⁴-(4-(methylamino)butyl)butane-1,4-diamine, **6b**, which contained three *N*-methylhomospermidine motifs. This PTI exhibited decreased sensitivity to amine oxidases and low toxicity as well as high potency ($EC_{50} = 1.4 \mu\text{M}$) in inhibiting the uptake of spermidine ($1 \mu\text{M}$) in DFMO-treated L3.6pl human pancreatic cancer cells.



INTRODUCTION

Polyamines are essential growth factors for cells and play key roles in transcription, translation, and chromatin remodeling.¹ Intracellular polyamine homeostasis is maintained by a balance between polyamine biosynthesis, degradation and transport.^{1d} The polyamine transport system (PTS) is an important target, as many cancer cell types readily import polyamines to sustain their growth rate, especially in the presence of polyamine biosynthesis inhibitors such as difluoromethylornithine (DFMO).^{1a–d,2} Numerous tumor types have been shown to contain elevated polyamine levels and have active transport systems to import exogenous polyamines.^{1a} These cancer cell properties facilitate the cell-selective delivery of polyamine–drug conjugates to cancer cell types.^{1a–d,2}

Many cancer cell types have been shown to have high intracellular polyamine levels, which are acquired via either polyamine biosynthesis or import pathways. A balance is maintained between these two processes, and there are cellular feedback mechanisms to guard against intracellular polyamine overload (e.g., antizyme induction).^{1c} One of the key enzymes involved in polyamine biosynthesis is ornithine decarboxylase (ODC). For cancer cells, ODC is often up-regulated in an effort to increase the intracellular pools of polyamines via the biosynthetic pathway, and ODC itself is considered a proto-oncogene.³ Early efforts to control cell growth led to the development of DFMO as a suicide inhibitor of ODC.^{4a–c} Despite the success of DFMO as an ODC inhibitor, DFMO-

treated cells often up-regulate polyamine transport activity to replenish their depleted intracellular polyamine pools. This shortcoming of DFMO therapy has prompted the development of polyamine transport inhibitors (PTIs) in an attempt to block the compensatory response of up-regulated polyamine import.

Prior studies by Ask et al. in 1992 demonstrated that DFMO modestly increased the survival time of mice treated with murine leukemia L1210 cells and a low polyamine diet.⁵ In contrast, DFMO provided 30–75% cures in leukemic mice bearing mutant L1210-MGBGr cells, which were deficient in polyamine transport.⁵ This work provided evidence that inhibition of polyamine transport by genetic means could potentiate the effects of DFMO and provide cures. In theory, such an outcome can also be obtained using DFMO in combination with a small molecule which acts as polyamine transport inhibitor (PTI).

Indeed, the combination therapy of DFMO+PTI can be very effective in depleting intracellular polyamine levels and limiting tumor growth. For example, Burns et al have demonstrated the utility of a lysine-spermine conjugate (D-Lys-Spm, MQT 1426, **1a**, Figure 1) in combination with DFMO, in vitro.⁶ The D- and L- enantiomers (**1a** and **1b**) gave similar performance in vitro.⁷ This combination therapy was also demonstrated in cats with oral squamous cell carcinoma.⁸ In 2009, these investigators

Received: August 1, 2013

Published: January 9, 2014

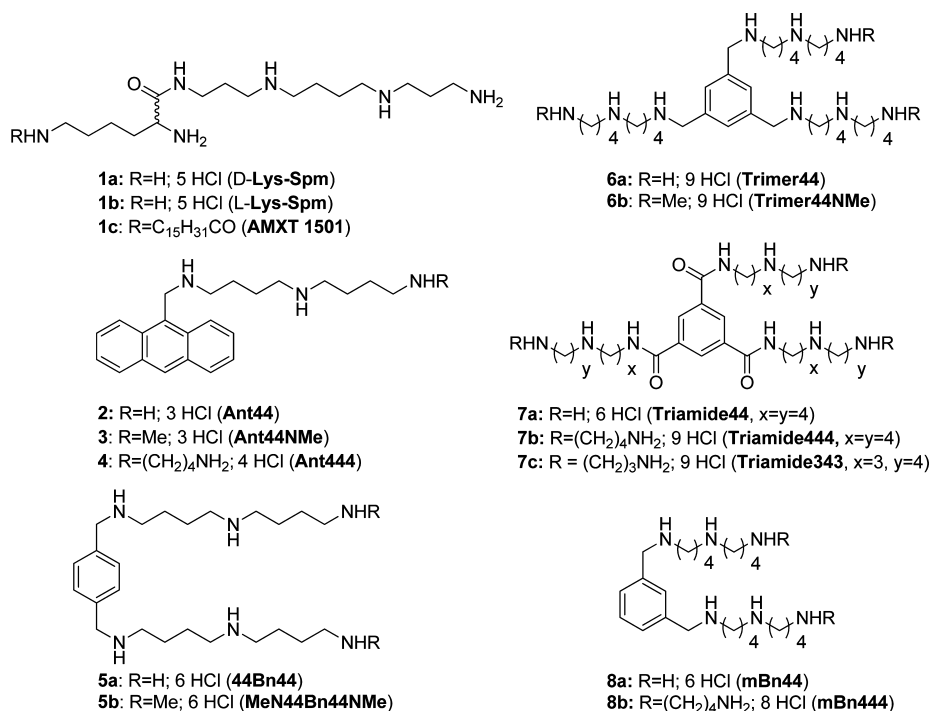


Figure 1. Structures of polyamine-transport-targeting compounds 1–8.

reported significant improvements in potency by adding a C₁₆ lipophilic substituent to their design (**1c**).⁷ This improved PTI (**1c**) was used in combination with DFMO in the treatment of squamous cell carcinomas (SCC) in a transgenic ODC mouse model of skin cancer, and 88% of SCCs showed complete or nearly complete remission. These promising results suggested that further optimization of the DFMO+PTI strategy was warranted.

A major impediment to PTI design, however, is our limited knowledge of the mammalian polyamine transport system itself. While genes associated with polyamine transport have been described in lower organisms (e.g., *E. coli* and *C. elegans*), the genes involved in mammalian transport are only now being identified.⁹ As result, most of our understanding of the PTS stems from phenotypical observations, relative kinetic uptake studies, and structure–activity relationships.

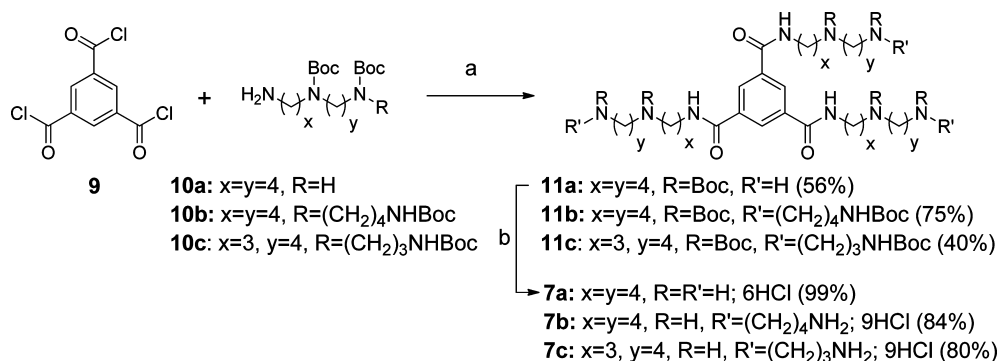
Two models of mammalian polyamine transport have been proposed by Poulin¹⁰ and Belting¹¹ and were recently updated by Gerner to include findings with Caveolin-1, nitric oxide synthase 2 (NOS2), and SLC3A2.^{9f} Poulin suggested that polyamines enter the cell through an active plasma membrane transporter, followed by sequestration into polyamine-sequestering vesicles (PSVs).^{10b} In order for polyamines to internalize within these PSVs, a vesicular H⁺/polyamine carrier is needed to facilitate the import and escape from the PSV.^{10b} Belting, on the other hand, suggested a multistep endocytotic process where polyamines bind to heparan sulfate proteoglycans in caveolae.^{11b} Once bound, the polyamines are then endocytosed via a caveolin-dependent process and their heparan sulfate chains are subsequently cleaved and further processed by NO to liberate the polyamines.^{11b} Heparan sulfate is a proteoglycan with an architecture that has carboxylate and sulfate groups separated by discrete distances. This is consistent with known observations where the number of charges and distances separating the cationic charges on the polyamine substrate all influence polyamine-binding events and uptake.^{2c–e,12} These

two models are not mutually exclusive and may operate in tandem or in concert to maintain polyamine homeostasis.

Beyond these two models, it is currently unclear how the recently discovered genes^{9g} involved in mammalian polyamine transport operate and how they control these or other polyamine uptake processes. Indeed, this area is ripe for further investigation, and the development of potent PTIs which target specific or several polyamine transport pathways will be of great value to investigators interested in polyamine-transport processes and further exploration of the existing models. The present study explores the potency and performance of PTIs with multiple polyamine arms with the goal to provide new molecular tools for investigating polyamine transport.

The polyamine transport system (PTS) has shown wide structural tolerance for importing N-substituted-polyamine derivatives. Monosubstituted systems such as **2–4** were effective PTS ligands; however, disubstituted analogues such as **5a** were more superior PTS ligands (Figure 1).^{2c–e,13} In this regard, compounds which contain preferred polyamine sequences often readily interact with the PTS.^{2c,d} Recent work has also shown that the number of appended polyamine chains is important. For example, the disubstituted benzene derivative **5a** is a potent transport ligand and is highly toxic, whereas the trisubstituted derivative **6a** is a potent PTI and is relatively nontoxic.

Compounds **5a** and **6a** illustrate two scaffolds, which can display PTI activity. First, a selective PTS ligand such as **5a** with high affinity for the PTS can readily out-compete the native polyamines for the putative cell surface receptors and theoretically function as an effective PTI. The transported ligand **5a** can also enter and kill the cell. The toxicity of **5a**, however, becomes dose-limiting for in vitro experiments designed to assess the PTI activity of **5a**. Disubstituted analogue **5a** had a low K_i value in L1210 murine leukemia cells (0.52 μM) and a L1210 IC₅₀ value of 0.16 μM. Even though compounds such as **5a** which target, enter, and kill cells

Scheme 1.^a

^aReagents: (a) K_2CO_3 , Aliquat, CH_2Cl_2/H_2O ; (b) 4 M HCl, EtOH.

via the PTS have clear value, they were undesirable as PTIs because of high toxicity.^{13b}

Our goal was to develop PTIs with low toxicity, which could ultimately be given chronically to patients in combination with DFMO. The trisubstituted derivative **6a** illustrates a second paradigm, which involves the use of a ligand with high affinity for the polyamine transport system with low cellular toxicity. This type of design is preferred, as one avoids the toxicity constraints of **5a**. For example, **6a** had virtually the same K_i value as **5a** in L1210 murine leukemia cells (**5a**: 0.52 μM , **6a**: 0.49 μM) but a dramatically higher L1210 IC_{50} value (**5a**: 0.16 μM , **6a**: 122 μM). In short, the trisubstituted system **6a** was over 760-fold less toxic than the disubstituted system **5a**.

Recent efforts with **6a** also demonstrated its high IC_{50} values ($IC_{50} > 100 \mu M$) in CHO and CHO-MG cells.^{13b} Compound **6a** also blocked the uptake of a PTS-selective probe, Ant44 (**2**), into CHO cells.^{13b} These promising findings for **6a** provided the impetus for the current study to further improve its design. While the area of PTI development has recently been reviewed in detail,¹⁴ this report describes our efforts to develop nontoxic PTIs predicated upon the novel trisubstituted design of **6a**.

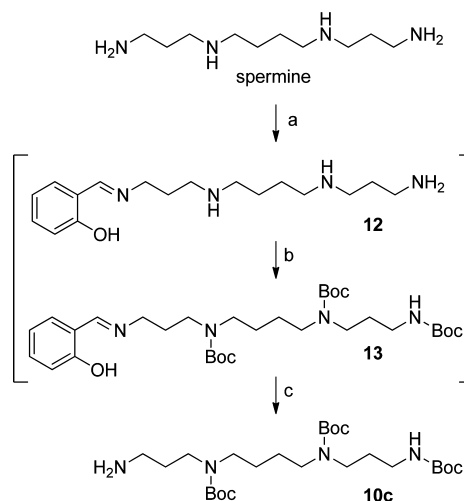
RESULTS AND DISCUSSION

The observation that trisubstituted **6a** was relatively nontoxic PTI whereas the 1,4-disubstituted system **5a** was a toxic PTS ligand led to key questions which needed to be addressed. Which structural component of **6a** was responsible for its low toxicity: (a) the 1,3-substitution pattern or (b) the presence of the third polyamine substituent? These questions were addressed via the synthesis and bioevaluation of the triamide systems **7a-c** (Figure 1) and the meta-substituted benzene ring compounds (**8a** and **8b**). Using these model systems, we were able to clearly demonstrate that the third polyamine substituent was responsible for the low toxicity of **6a**. This insight was then extended to include the *N*-methyl derivative **6b**, which had even lower toxicity, decreased sensitivity to amine oxidases, and potency similar to that of **6a**. In summary, these studies provided a nontoxic, potent PTI **6b** for future use in combination with DFMO in vivo.

Synthesis. The synthesis and characterization of 1,3,5-trisubstituted derivative **6a** has been previously described by Kaur et al.,^{13b} and the synthesis of L-lysine-spermine conjugate **1b** was previously described by Burns et al.¹⁵ These compounds, **1b** and **6a**, were resynthesized for comparison purposes in vitro with the new PTIs.

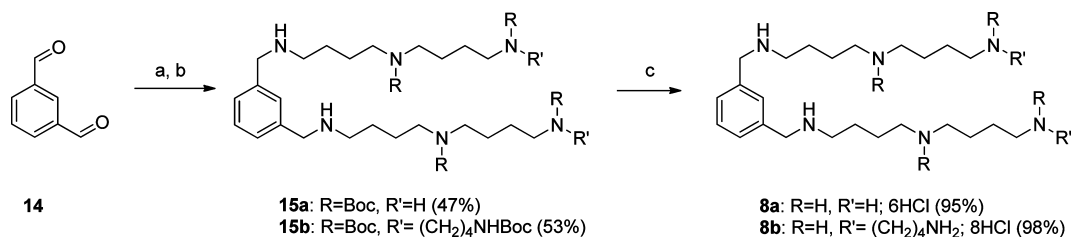
The impetus for making triamide **7c** was based upon the fact that the planned amide examples, **7a** and **7b**, incorporated non-native polyamine sequences (e.g., homospermidine). We speculated that the use of the native polyamine, spermine, could provide a triamide-containing PTI (**7c**) with lower toxicity. Indeed, significant changes in toxicity have been observed in derivatives containing subtle changes in their polyamine sequence.^{13a} The new conjugates **7a-c** were also synthesized to better understand how the attachment of the polyamine to the aryl core affected toxicity and potency.

As shown in Scheme 1, synthesis of these novel PTIs (**7a-c**) required the synthesis of the known Boc-protected polyamines (**10a-c**).^{2d,16,17} While **10a** and **10b** were generated in successive steps from 4-bromobutyronitrile and mono-Boc-protected putrescine using established methods,¹⁶ the spermine adduct was made by an alternative route directly from spermine using salicylaldehyde (1 equiv) as shown in Scheme 2.¹⁸

Scheme 2^a

^aReagents: (a) 2-Hydroxybenzaldehyde; (b) di-*tert*-butyl dicarbonate; (c) CH_3ONH_2/Na_2CO_3 (45% yield after three steps).

Formation of the salicylimine occurred at the primary amine sites. This allowed for easy introduction of Boc groups to the remaining three amine centers of spermine in situ to give **13**. Subsequent hydrolysis of the imine **13** with methoxyamine gave the desired tri-Boc-protected spermine **10c** in 45% yield after three steps. This process has significant advantages in yield and

Scheme 3^a

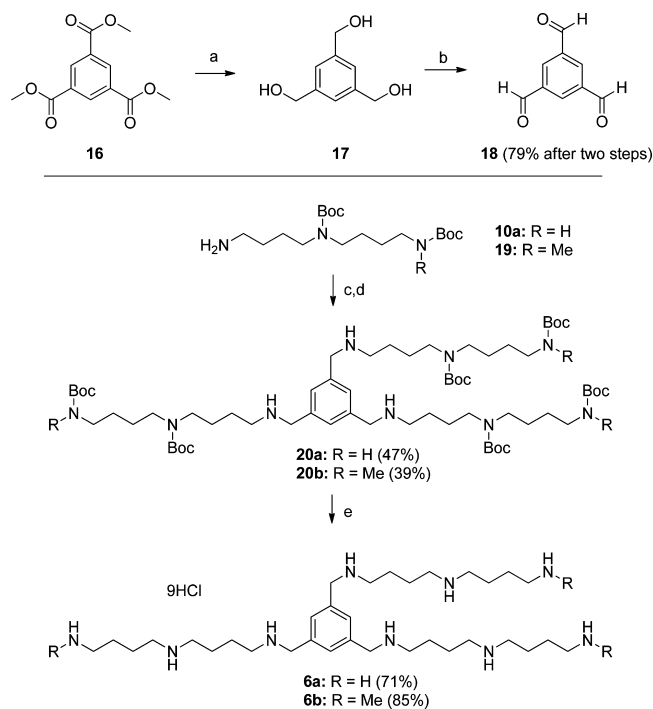
^aReagents: (a) 25% MeOH/CH₂Cl₂, Boc-protected amine 10a or 10b; (b) 50% MeOH/CH₂Cl₂, NaBH₄; (c) 4 M HCl, EtOH.

time over other methods due to the availability of spermine versus the multistep construction of the 3,4,3-triamine sequence using omega bromoalkanonitriles and acrylonitriles.¹⁹ Each of the three amines 10a–c were then coupled to the commercially available 1,3,5-benzenetricarboxylic acid chloride 9 under biphasic conditions to give the respective triamides 11a–c in moderate yield (56%, 75%, and 40%, respectively, Scheme 1). Triamides 11a–c were then deprotected to give the respective compounds 7a–c in high yield, respectively.

Disubstituted derivative 8a was generated to determine if the third polyamine substituent present in 6a was necessary for PTS inhibition and provided a control to determine whether meta-substitution contributed to the reduced toxicity observed with 6a (via comparisons with 8a and 5a). In addition, 8b was synthesized to evaluate how extending the polyamine sequence and number of charges presented to the putative cell-surface receptor affected PTI performance. The two-arm platforms were synthesized from the starting 1,3-dialdehyde 14, which was commercially available.^{13b} As shown in Scheme 3, the synthesis began with the reductive amination of aldehyde 14 with the corresponding protected polyamine (10a or 10b) to yield compounds 15a and 15b, respectively.¹⁶ Deprotection then gave the meta-substituted systems 8a and 8b in 44% and 51% overall yield after two steps, respectively.

The above compounds were generated for comparisons to the known PTIs 6a and 1b. In addition, prior work in our lab with 2 and its *N*-methyl analogue 3 demonstrated that *N*-methylation led to polyamine drugs with lower toxicity and improved stability toward amine oxidases.^{17a} This same trend was also recently observed in the related disubstituted systems, e.g., 5a vs 5b.^{13b} Therefore, we elected to also apply the *N*-methylation technology to our trisubstituted PTI design in an effort to generate a PTI 6b with lower toxicity and improved stability.

As shown in Scheme 4, the synthesis of 6b began with the synthesis of triol 17 from the commercially available triester 16 using LiAlH₄. Attempts to oxidize triol 17 to aldehyde 18 with pyridinium dichromate (PDC) at room temperature gave incomplete reactions. IBX was found to be superior in this regard and gave 79% yield after both steps (reduction/oxidation).²⁰ Subsequent coupling of aldehyde 18 with the known Boc-protected *N*¹-methylhomospermidine derivative 19^{13b} gave trisubstituted adduct 20b (39%) which was then converted to 6b (85%) with 4 M HCl. Note: the related 6a was made from 20a by a similar route using 18 and 10a.^{13b} The yields obtained for 6a (71%) and its intermediate 20a (47%) during their resynthesis^{13b} are listed in Scheme 4 for completeness. The synthesis of the starting amines 10a and 19 have been previously described.^{16,13b}

Scheme 4^a

^aReagents: (a) LiAlH₄/THF; (b) IBX/*tert*-butyl alcohol; (c) 18 in 25% MeOH/CH₂Cl₂; (d) 50% MeOH/CH₂Cl₂/NaBH₄; (e) 4 M HCl/EtOH.

Bioevaluation of these compounds was then conducted using a series of assays designed to compare the ability of each compound to target the PTS of mammalian cells.

CHO and CHO-MG* Studies. Chinese hamster ovary (CHO) cells were chosen along with a mutant cell line (CHO-MG*) to comment on how the synthetic conjugates gain access to cells.^{2c–e,21} The CHO-MG* cell line is polyamine-transport deficient and represents a model for alternative modes of entry (other than the PTS) including passive diffusion or use of another transport system. The wild-type CHO cell line, on the other hand, represents cells with high polyamine transport activity.²² A comparison of toxicity in these two CHO cell lines provided a screen that would detect selective use of the PTS. High utilization of the PTS by the polyamine compounds would be very toxic to CHO cells. However, reduced toxicity would be expected in CHO-MG* cells due to its limited transport activity.^{2c} A CHO-MG*/CHO IC₅₀ ratio was determined for each compound, and a high CHO-MG*/CHO ratio was expected for highly PTS-selective compounds. The results for this screen are listed in Table 1. The published

Table 1. Biological Evaluation of Polyamine Derivatives (1b, 5a, 6–8) in CHO and CHO-MG* Cells^{a-c}

compound	CHO IC ₁₀ (μM) ^b	CHO EC ₅₀ (μM) ^c	CHO-MG* IC ₅₀ (μM)	CHO IC ₅₀ (μM)	CHOMG*/CHO IC ₅₀ ratio ^d
1b (L-Lys-Spm)	>100	1.37	>100	>100	ND
5a (44Bn44)	0.001	NA	19.6 (±0.8)	0.027 (±0.001)	727
6a (Trimer44)	10	0.34	66.9 (±6.2)	>100	ND
6b (Trimer44NMe)	10	0.42	>100 ^e	>100	ND
7a (Triamide44)	>100	60	>100	>100	ND
7b (Triamide444)	1	NA	69.1 (±4.0)	16.0 (±0.7)	4.3
8a (mBn44)	0.01	NA	30.0 (±0.8)	0.028 (±0.002)	1072
8b (mBn444)	0.01	NA	13.4 (±0.8)	0.04 (±0.007)	335

^aCHO and CHO-MG* cells were incubated with 1 mM AG for 24 h prior to compound addition. ^bThe IC₁₀ value represents the highest concentration of compound which resulted in ≤10% cell growth inhibition (i.e., ≥90% cell viability) vs an untreated control over the same time period (48 h). ^cThe EC₅₀ value is the concentration of the PTI compound needed to reduce the cell viability halfway between the % viability observed with DFMO+Spd control and the % viability observed for the DFMO-only control (DFMO IC₅₀ CHO: 4.2 mM). (Note: these are illustrated in Figure 3 as the green and red lines, respectively). These values are listed here in Table 1 for completeness and comparison to the other properties observed in CHO cells. The listed value is the EC₅₀ value for the respective PTI in its corresponding DFMO+Spd+PTI experiment in CHO cells. ^dA high CHO-MG*/CHO IC₅₀ ratio indicates a compound with high utilization of the PTS to enter and kill cells. ^eThe CHO-MG* IC₅₀ of 6b was 121.7 (±3.9) μM. Note: compound 7c was not evaluated in CHO but was evaluated in L3.6pl cells (Table 2). Note: Cells were incubated for 48 h at 37 °C in 5% CO₂ with the respective conjugate. All experiments were in triplicate. ND: not determined because of low toxicity in both CHO cell lines. NA: not applicable.

PTI (Lys-Spm, 1b) was synthesized and included as a positive control.^{6,7,15,23}

The CHO-MG* line was derived from the original CHO-MG line obtained from Flintoff et al.^{22a,24} and provided similar results with numerous previously synthesized controls.^{17b} For example, the respective CHO-MG/CHO IC₅₀ ratios for previously synthesized polyamine-anthryl conjugates, 2 and 5a were 148¹² and 677,^{13b} whereas the CHO-MG*/CHO IC₅₀ ratios of 2 and 5a were 43 and 727, respectively.^{17b} As the original stocks of CHO-MG were no longer available from their original source, CHO-MG* were used in the PTS screen.

As shown in Table 1, the IC₁₀ value of each compound was determined in CHO cells. The IC₁₀ value represents the highest concentration of compound which resulted in ≤10% cell growth inhibition (i.e., ≥90% cell viability) vs an untreated control over the same time period. At its IC₁₀ value, the compound was deemed essentially nontoxic. The IC₁₀ value provided the highest dose at which the PTI could be added to the cell culture and not result in a significant cytotoxic response (due to its own intrinsic toxicity). This was important as the assay used to assess PTI function measured decreases in cell viability.

The IC₅₀ value was the concentration of the compound which resulted in 50% cell growth inhibition vs an untreated control over the same time period. For example, a compound with a low IC₅₀ value (e.g., 5a: CHO IC₅₀=0.027 μM) was considered to be more toxic to CHO cells than 6a (IC₅₀>100 μM). The IC₅₀ values for each compound were determined in CHO and CHO-MG* cells, and the CHO-MG*/CHO IC₅₀ ratio was used to assess the ability of the compound to enter and inhibit growth of the cell via the PTS. PTS-selective compounds such as 5a, 8a, and 8b had high CHO-MG*/CHO IC₅₀ ratios and were considered very selective in entering and inhibiting the growth of cells with active polyamine transport systems. These compounds were also competitive inhibitors of polyamine transport, and exogenous spermidine has been shown to rescue cells treated with 5a.^{17b} While these compounds may be of interest for targeting cancers via their PTS, the goal here was to identify nontoxic PTIs and not lethal PTS-targeting compounds.^{17b}

The 1,3,5-trisubstituted analogues 6a and 6b exhibited very high IC₅₀ values in CHO cells (>100 μM) and were deemed relatively nontoxic. In stark contrast, the 1,4-disubstituted

derivative 5a was very toxic (CHO IC₅₀: 0.027 μM). Thus, 6a and 6b were found to have >3700 fold lower toxicity in CHO cells than 5a. A similar result was found previously in murine leukemia L1210 cells, where 6a was found to be >760 fold less toxic than 5a in L1210 cells (L1210 IC₅₀: 6a = 122.3 μM and 5a = 0.16 μM). These two compounds, however, possessed nearly identical K_i values in L1210 cells (5a: 0.52 μM ± 0.11 and 6a: 0.49 μM ± 0.02, respectively),^{13b} indicating that these two compounds bind to the L1210 PTS recognition elements with nearly equal affinity.

Given the dramatic differences in toxicity and similar binding affinities of 5a and 6a, we speculated that only two of the polyamine arms may interact with the putative cell surface receptor. This idea was investigated via additional studies to test whether the third polyamine arm or the meta substitution pattern of 6a was responsible for the lower toxicity of 6a compared to 5a.

The control compound 8a, which contained two polyamine arms in a 1,3-substitution pattern, provided a model system to address this issue. If the third polyamine arm was required for low toxicity, then the two-arm moiety 8a would be a potent PTS targeting compound with high toxicity. If a meta substitution pattern was critical for low toxicity, then 8a would have low toxicity. Of these two possible outcomes, we found the former to be the case.

Indeed, evaluation in CHO and CHO-MG* cells proved to be very interesting. Compound 8a had nearly identical toxicity as 5a (CHO IC₅₀ 8a: 27 nM; 5a: 28 nM) and 8a was the most PTS selective of the series (e.g., CHOMG*/CHO IC₅₀ ratio: 1072 in Table 1). This finding strongly suggested that the third polyamine arm of 6a was in large part responsible for the low toxicity of 6a in CHO cells. Note: 6a had >3500-fold lower toxicity than 8a in CHO cells.

The tetraamine analogue 8b was found to be less PTS selective (CHO-MG*/CHO IC₅₀ ratio: 335) than its counterpart, 8a (IC₅₀ ratio: 1072). This demonstrated that the longer polyamine message lowered the PTS selectivity of the design. This finding was also observed in the comparison of monosubstituted triamine 2 and tetraamine 4 (Figure 1), where triamine 2 was more PTS selective than tetraamine 4 in a related CHO/CHO-MG screen.^{2d} Indeed, triamine derivatives were found to be superior to tetraamines in terms of binding and entering cells via the PTS.^{13a}

A comparison of **8a** (meta) and **5a** (para) suggested that the meta substitution pattern enhanced the PTS targeting ability of the drug. This is observed in the higher CHO-MG*/CHO ratio for **8a** in Table 1. We hypothesized that this was due to the intrinsic preorientation of the appended polyamine arms in the meta-substituted system **8a**. Although the effect was cell line dependent, other authors have demonstrated that conformational constraint of the linker connecting two polyamine chains can impart significant differences in potency in PC-3, MCF7, and U251MG cells.²⁵ Therefore, we concluded that the polyamine sequence, the number of polyamine chains, and the orientation of these chains all influenced the PTS-targeting ability of these compounds and their associated toxicity profiles.

Compound **7a** presented a unique opportunity to evaluate a 1,3,5-substituted triamide platform as a PTI. The amide linkage in **7** removes the formal positive point charge at the ring attachment position. From the cationic charge perspective, triamides **7a** and **7b** represent architectures, which present three putrescine (**7a**) or three homospermidine (**7b**) "messages" to the putative cell surface receptors, respectively. The trends in compound toxicity were very insightful. As shown in Table 1, the IC₅₀ of **7a** was >100 μM, whereas the IC₅₀ of **7b** was 16 μM. In the comparative CHO and CHO-MG* screen, triamide **7b** demonstrated modest PTS selectivity (IC₅₀ ratio: 4.3) and the ratio for **7a** was not determined due to its low toxicity in both cell lines (Table 1).

In summary, the disubstituted systems (**5** and **8**) and the triamide **7b** containing the longer polyamine sequence were all found to be significantly more toxic than **6a** and **6b**. As discovered in subsequent studies, the relative toxicities of these compounds significantly influenced the doses that could be used in combination with DFMO.

DFMO CHO Studies. Inhibition of ODC by DFMO can lead to an increase in polyamine transport activity to maintain intracellular polyamine homeostasis (see Figure 2). The high

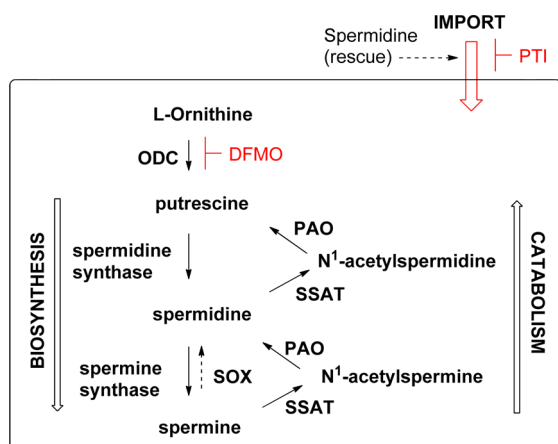


Figure 2. Overview of polyamine metabolism and the combination therapy of DFMO+PTI. ODC: ornithine decarboxylase, SOX: spermine oxidase, PAO: polyamine oxidase, SSAT: spermidine-spermine acetyl transferase. The combination therapy of DFMO+PTI is expected to generate sustained intracellular polyamine depletion, as both biosynthesis and import should be inhibited. In the absence of a PTI, exogenous spermidine can enter and rescue DFMO-treated cells. This rescue effect is due to biosynthetic and catabolic processes which can interconvert each of the native polyamines (e.g., spermidine, Spd) to each of the other native polyamines as needed.

transport activity of DFMO-treated CHO cells was used to assess the PTI activity of the new compounds. Specifically, we investigated the ability of each compound to block the entry of a rescuing dose of spermidine (1 μM) in DFMO-treated CHO cells.^{15,23} This method required the determination of three parameters before running the definitive assay. First, the 48 h IC₅₀ value of DFMO was determined in CHO cells (DFMO 48 h IC₅₀ in CHO: 4.2 mM). Second, CHO cells were treated with the IC₅₀ dose of DFMO, and the minimum amount of spermidine (Spd) needed to rescue these DFMO-treated cells back to their maximum viability (>90% viability in this cell line) was determined. In CHO cells, spermidine at 1 μM was sufficient to rescue the DFMO-treated CHO cells. Third, the 48 h IC₁₀ value was determined for each compound. The first two parameters defined the DFMO and Spd concentrations to be used, and these remained fixed throughout the assay. The third parameter (IC₁₀ value) defined the upper limit of the concentration of the PTI agent that could be used in the DFMO+Spd+[PTI] experiment without introducing significant toxicity from the PTI agent itself to the DFMO+Spd-treated cells. Control experiments with Spd and PTI (without DFMO) revealed that no synergistic toxicity was induced by these two polyamine compounds when dosed together in CHO cells. In this manner, we could be confident that the results obtained were due to the ability of the compound to block spermidine entry and was not due to PTI toxicity or unexpected Spd+PTI toxicity. The fact that the active compounds had EC₅₀ values significantly below the compound's IC₁₀ value provided further support for this approach.²⁶

We found that PTI potency was best evaluated through the use of spermidine (Spd). Spermidine was found to effectively rescue L1210 and CHO cells from polyamine-based drugs and DFMO.²⁸ We noted that the K_m values of the native polyamines (Put, Spd, Spm) were 208.2, 2.46, and 1.34 μM, respectively, in L1210 cells.^{2d} Thus, any of the three native polyamines could theoretically be used as a rescue agent in DFMO-treated cells because of the cell's ability to interconvert internal polyamine pools (see Figure 2). Putrescine transport was easily blocked, however, because of its high K_m value, and spermine at high doses was toxic to cells.^{2d} In this regard, spermidine was more challenging to inhibit than putrescine, was less toxic to cells than spermine, and was thus preferred as the competing native polyamine in our system.

A nontoxic PTI would be expected to inhibit Spd entry, and the cell treated with DFMO+Spd+PTI would be expected to resemble cells treated with DFMO only, i.e., with ~50% viability. With this assay in place, the effectiveness of each potential PTI was tested and compared. In a 96-well plate format, CHO cells were treated with an IC₅₀ dose of DFMO (4.2 mM), a fixed concentration of Spd (1 μM), and increasing doses of the PTI compound (from 0 μM to its approximate IC₁₀ value). The cells were then incubated for 48 h at 37 °C.

Sample results are shown in Figure 3 for **6a** and **6b**. The EC₅₀ value is the concentration of the PTI compound needed to reduce the cell viability halfway between the % viability observed with DFMO+Spd control (green line in Figure 3) and the % viability observed for the DFMO-only control (red line). The EC₅₀ values for **1b**, **6a**, **6b**, and **7a** were 1.37, 0.34, 0.42, and 60 μM, respectively, and are listed in Table 1. In each case, the EC₅₀ value was well below the IC₁₀ value of the compound tested, and the innate toxicity of the PTI compound was, therefore, excluded as a major contributing factor to the results obtained.

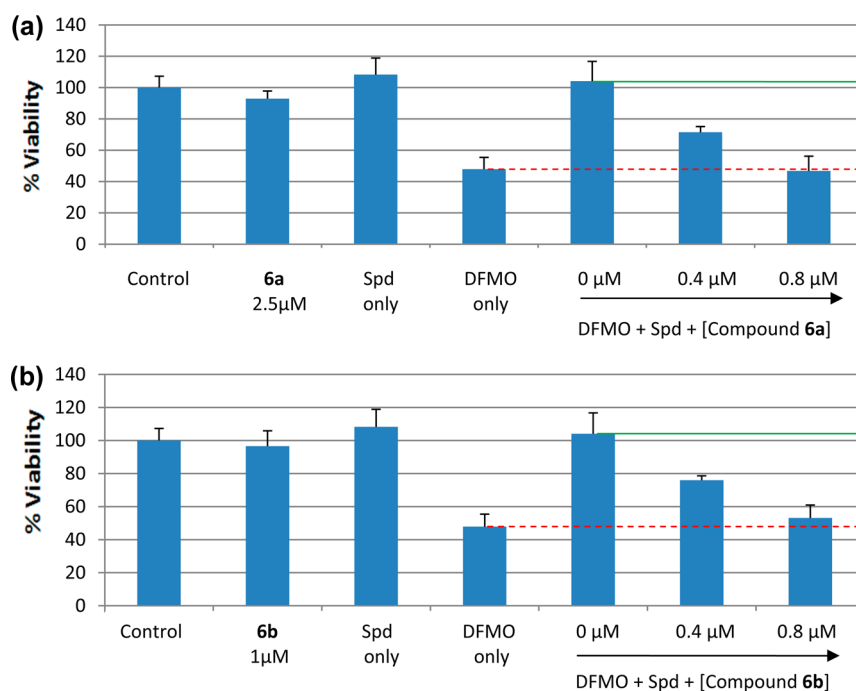


Figure 3. Ability of (a) **6a** (Trimer44) and (b) **6b** (Trimer44NMe) to prevent Spd rescue of DFMO-treated CHO cells. Cells were incubated for 48 h at 37 °C with the respective conjugate, DFMO (4.2 mM), and Spd (1 μM). A 1 mM AG solution was incubated with cells for 24 h prior to drug addition. Column 1 is the untreated CHO control, column 2 shows the % relative cell viability when dosed with PTI only at or above the concentrations tested in the figure and shows that the PTI is nontoxic at the tested doses, column 3 is the Spd-only control at 1 μM, column 4 is the DFMO-only control at 4.2 mM, and columns 5–7 have fixed concentrations of DFMO (4.2 mM) and Spd (1 μM) with increasing concentrations of PTI as indicated in each lane. The PTIs at their IC₁₀ values when tested alone gave ≥90% viability as determined in separate control experiments; the respective IC₁₀ values are listed in Table 1. Because of the high potency of **6a** and **6b**, they only needed to be dosed to 0.8 μM to illustrate their respective dose dependence as a PTI agent. Note: this effective concentration was significantly below the IC₁₀ value of both **6a** and **6b** (10 μM).

Table 2. Biological Evaluation of Polyamine Derivatives (1b and 6–8) in L3.6pl Cells^{a–e}

compound	K _i (nM) ^d	L3.6pl IC ₁₀ (μM)	EC ₅₀ in DFMO+Spd+PTI expt (μM)	L3.6pl IC ₅₀ (μM)
1b (L-Lys-Spm)	26	>100	1.06	>100 ^f
6a (Trimer44)	36	10	0.77	>100
6b (Trimer44NMe)	55	10	1.40	>100
7a (Triamide44)	398	>100	89.8	>100
7b (Triamide444)	ND	1	NE	9.7 (±0.5)
7c (Triamide343)	ND	8	NE	47.5 (±2.1)
8a (mBn44)	ND	0.1 ^e	NE	52.2 (±2.0)
8b (mBn444)	ND	0.01 ^e	NE	7.5 (±0.4)

^aL3.6pl cells were incubated with 250 μM AG for 24 h prior to drug addition. ^bFor experiments other than the K_i determinations, L3.6pl cells were incubated for 48 h at 37 °C with the respective conjugate. ^cAll experiments were performed in triplicate. ^dK_i values were determined via ³H-spermidine uptake measurements taken over 15 min at 37 °C, and the K_m of Spd in L3.6pl cells was determined to be 666 nM. ^e**8a** (0.1 μM) and **8b** (0.01 μM) displayed viability within 8% of the untreated control. ND = not determined; NE = not effective when dosed at its IC₁₀ value. ^fThe L3.6pl IC₅₀ value for **1b** was >500 μM. DFMO (8 mM) and Spd (1 μM) were used in the EC₅₀ experiments.

As seen in Figure 3, compounds **6a** and **6b** effectively blocked the import of Spd (1 μM) in a dose-dependent fashion. For example, in Figure 3a, increasing levels of **6a** provided decreased viability in the presence of a fixed concentration of DFMO and Spd. Direct comparisons of **1b**, **6a**, **6b**, and **7a** in CHO cells (see Table 1) demonstrated that compounds **6a** and **6b** were excellent inhibitors of Spd import. Using the EC₅₀ values of **1b**, **6a**, **6b**, and **7a** in CHO cells as listed in Table 1, **6a** was 4-fold more potent than **1b** and 176-fold more potent than **7a** in the CHO spermidine rescue assay.

The high toxicity of compounds **7b**, **8a**, and **8b** was reflected in their low IC₁₀ values, which severely limited the amount of these compounds that could be dosed to CHO cells with no toxicity. In this regard, a toxic compound such as **8a**, which could only be dosed up to 0.01 μM (its IC₁₀), was ineffective in

inhibiting the uptake of spermidine. This was not surprising because the low IC₁₀ value of **8a** (0.01 μM) imparted a severe disadvantage on a molar basis in terms of its ability to outcompete Spd (1 μM) for the PTS. In CHO cells, **7b** could only be tested up to 1 μM, while **8a** and **8b** could only be tested up to 0.01 μM. When tested up to their respective IC₁₀ value in DFMO-treated CHO cells, none of these toxic compounds (**7b**, **8a**, and **8b**) could effectively prevent the rescue effect of the added Spd (1 μM).

In summary, the CHO experiments clearly demonstrated that **6a** (trimer44) and **6b** (trimer44NMe) were more effective than the other two PTIs: **1b** (L-Lys-Spm) and triamide **7a**.

L3.6pl Pancreatic Cancer Cell Line Studies. There is a strong need for new medicines for pancreatic cancer, as the five year survival rate for patients with metastatic pancreatic cancer

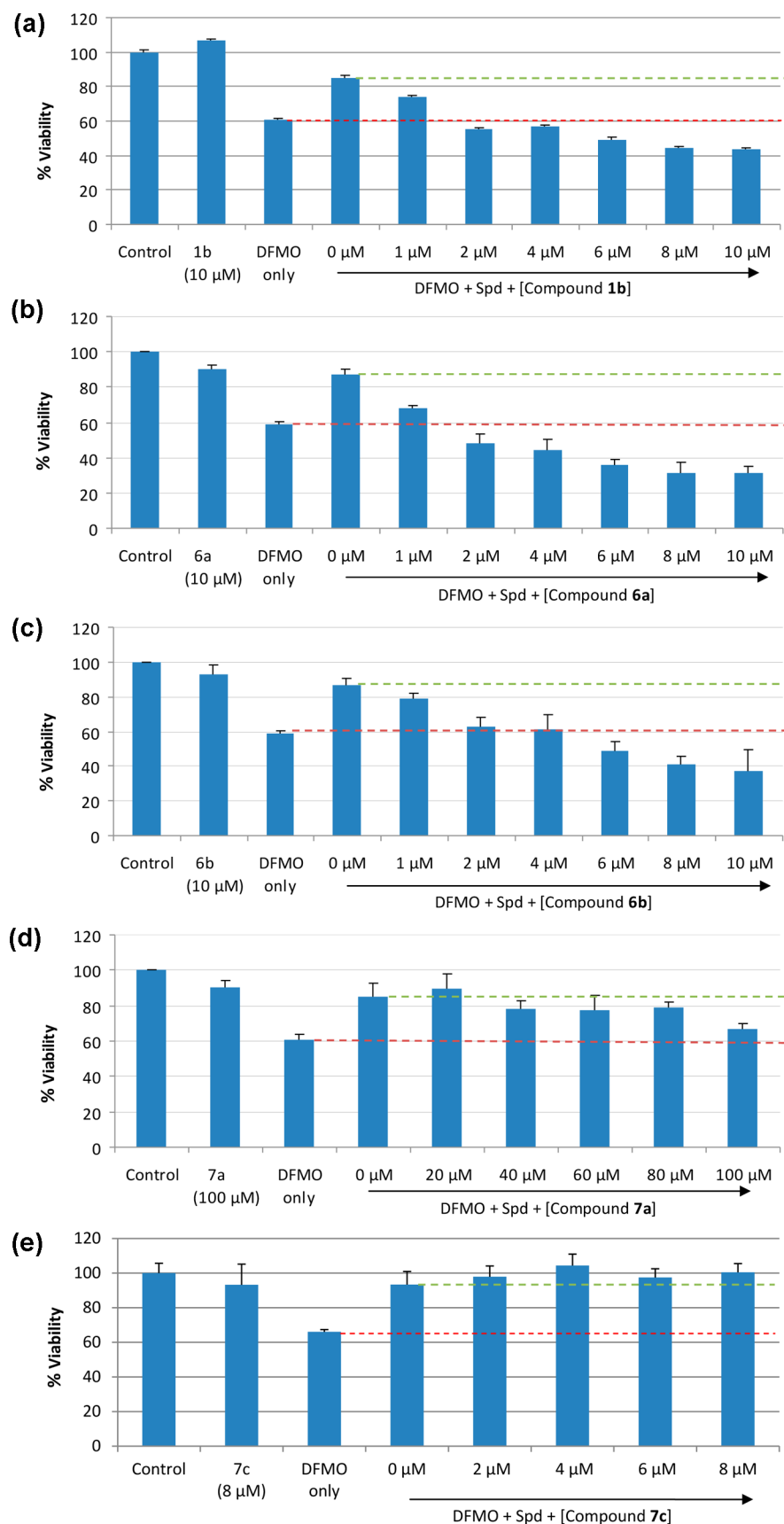


Figure 4. Ability of (a) **1b** (Lys-Spm), (b) **6a** (Trimer44), (c) **6b** (Trimer44-NMe), (d) **7a** (Triamide44), and (e) **7c** (Triamide343) to prevent Spd rescue of DFMO-treated L3.6pl cells. Cells were incubated for 48 h at 37 °C with increasing doses of the respective PTI, in the presence of fixed concentrations of DFMO (8 mM) and Spd (1 μ M). A 250 μ M solution of AG was incubated with cells for 24 h prior to compound addition. Column 1 is the untreated L3.6pl control, and column 2 shows the % relative cell viability when dosed with the PTI alone at the highest

Figure 4. continued

concentration tested in the figure and shows that the PTI is nontoxic. Note: the Spd-only control at 1 μM gave 100% viability (not shown), column 3 is the DFMO-only control at 8 mM, and columns 4–8 have fixed concentrations of DFMO (8 mM) and Spd (1 μM) with increasing concentrations of PTI as indicated in each panel. The EC_{50} could not be determined even at the IC_{10} value of **7c** (Figure 4e).

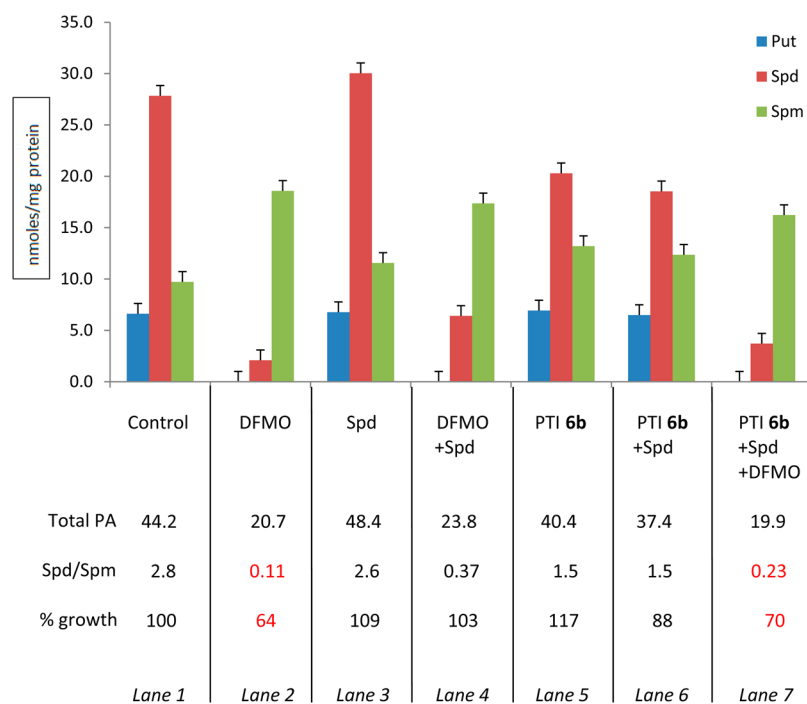


Figure 5. Intracellular polyamine levels in L3.6pl cells after 48 h incubation at 37 °C with DFMO (8 mM), Spermidine (Spd, 1 μM), or PTI **6b** (7 μM) alone or in combination. Total PA = total polyamine levels (putrescine+spermidine+spermine) expressed in nmol/mg protein. Spd/Spm = spermidine/spermine molar ratio. Conditions shown in red had appreciable growth reduction (DFMO only in lane 2 gave 64% growth vs untreated control, and the combination of **6b**+Spd+DFMO in lane 7 gave 70% growth). A 250 μM AG solution was incubated with cells for 24 h prior to compound addition.

is just 6%.²⁷ For this reason, the PTI panel was also evaluated in the metastatic human pancreatic cancer cell line, L3.6pl. The L3.6pl cell line²⁸ was chosen because of its *K-ras* mutation, which is prevalent in many human cancers and has been linked to increased polyamine uptake.²⁹ We were also interested in whether this pancreatic cell line, which was optimized for its high metastatic potential,²⁸ was sensitive to the DFMO+PTI combination therapy.

The IC_{50} values of the compounds in L3.6pl cells followed the same trend as seen in CHO (see Tables 1 and 2). First, the trisubstituted system **6a** was significantly less toxic than the disubstituted model **8a**. Second, increased polyamine length (**7a** vs **7b**, and **8a** vs **8b**) again led to increased toxicity. As a consistent trend in both CHO and L3.6pl cells, compounds **1b**, **6a**, **6b**, and **7a** were the least toxic PTIs tested (right column Table 2, all had IC_{50} values in L3.6pl cells >100 μM).

DFMO L3.6pl Studies. As performed previously with CHO cells, the 48 h IC_{50} of DFMO (8 mM), the minimum concentration of Spd needed to rescue DFMO-treated L3.6pl cells back to their maximum possible viability (typically 1 μM Spd gave 85–90% viability in L3.6pl cells), and the IC_{10} value of each compound were determined in L3.6pl cells (Table 2). Additionally, K_i values were determined to assess the relative affinity of each compound for the PTS and were obtained via uptake experiments over 15 min at 37 °C using ³H-spermidine and the most promising PTIs: **1b**, **6a**, **6b**, and **7a** (Table 2). Figure 4 illustrates the results obtained with **1b**, **6a**, **6b**, **7a**, and

7c in DFMO-treated L3.6pl cells. The low IC_{10} values of **7b** (1 μM), **8a** (0.1 μM), and **8b** (0.01 μM) again limited their ability to compete with Spd at 1 μM . As a result, when these toxic compounds (**7b**, **8a**, and **8b**) were tested at their respective IC_{10} values in L3.6pl cells, they were unsuccessful in inhibiting the uptake of Spd (1 μM , data not shown). Even though the IC_{50} values indicated that triamide **7c** (L3.6pl IC_{50} : 47.5 μM) was 4.9-fold less toxic than **7b** (9.7 μM), it was ineffective at its IC_{10} value (8 μM) in inhibiting Spd (1 μM) uptake in DFMO-treated L3.6pl cells (Figure 4e). These collective results are consistent with those found in the CHO experiments and further illustrated the need for PTIs with low toxicity (high IC_{10} values) and high potency. Along these lines, we noted the increased potency of **1b** in L3.6pl cells and low toxicity of **1b** in both CHO and L3.6pl cells, both of which were desirable PTI properties.

Because of potency and dosing issues, the EC_{50} values could only be determined for the compounds with IC_{10} values (≥ 10 μM) in L3.6pl cells. EC_{50} values for **1b**, **6a**, **6b**, and **7a** were 1.06 μM , 0.77 μM , 1.40 μM , and 89.8 μM , respectively. We noted that compounds **1b**, **6a**, and **6b** had low toxicity and were very effective PTIs in the L3.6pl cell line with IC_{50} values >100 μM and L3.6pl EC_{50} values ≤ 1.4 μM . Compound **7a** was also nontoxic (IC_{50} >100 μM) but was significantly less potent as a PTI (EC_{50} value = 89.8 μM). In this regard, compounds **1b**, **6a**, and **6b** had the optimal balance of low toxicity and low EC_{50} values. Rewardingly, the K_i values also tracked well with PTI

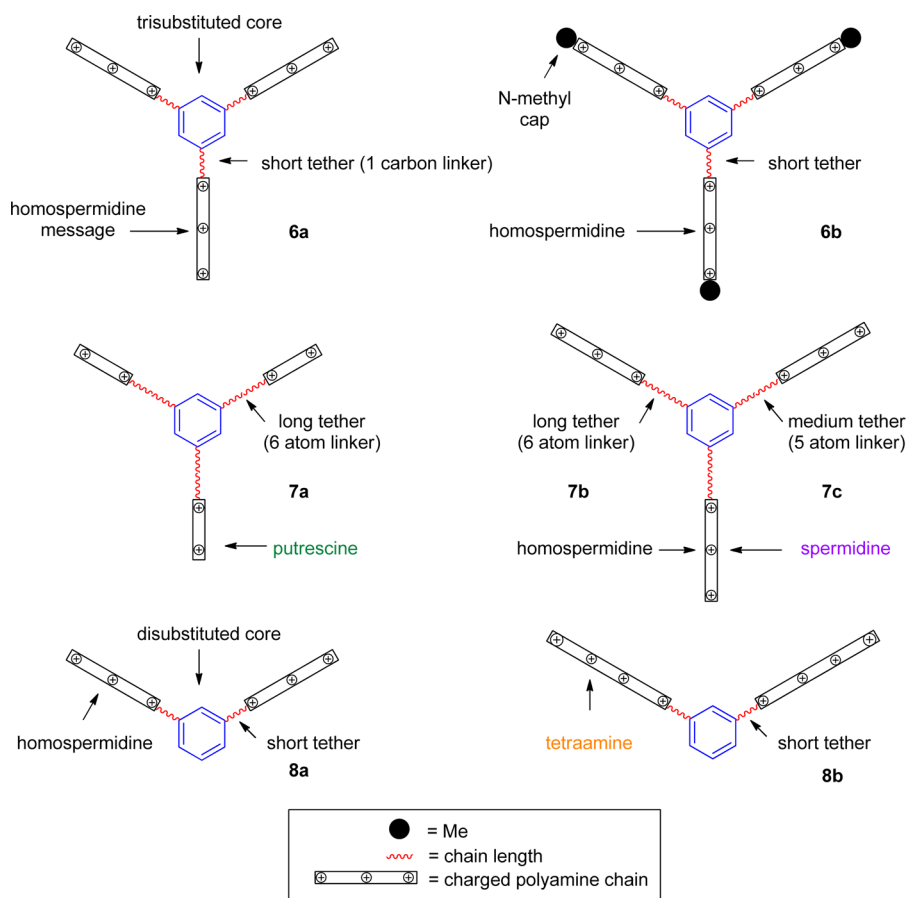


Figure 6. Design comparisons between 6–8.

performance (and EC_{50} values) with **1b**, **6a**, and **6b** having K_i values (≤ 55 nM) significantly lower than that of **7a** (398 nM, Table 2). These findings supported the competitive inhibition observed with these polyamine-containing compounds.

Intracellular Polyamine Levels. The effect of the combination therapy of DFMO+**6b** on the intracellular polyamine pools of L3.6pl cells was determined. As shown in Figure 5, putrescine levels were virtually undetectable and spermidine levels were dramatically reduced in each experiment when the ODC inhibitor DFMO was used at its 48 h IC_{50} concentration (8 mM). In contrast, spermine levels were maintained or increased in each experimental condition evaluated. This is consistent with other studies of DFMO, where cells tended to maintain or increase their spermine pools when challenged with DFMO or DFMO in combination with a PTI.^{4a,30,23} Compound **6b** was treated at five times its EC_{50} concentration ($EC_{50} = 1.4$ μ M), which was below its IC_{10} value (10 μ M) and was, therefore, not toxic at the concentration used (7 μ M).

Several interesting trends were apparent. First, the PTI **6b** showed reductions in intracellular spermidine levels (27% decrease) when dosed alone (Figure 5: lane 5) or in combination with exogenous spermidine (33% decrease, lane 6). The combination therapy of DFMO+PTI **6b** in the presence of a potential rescuing dose of spermidine (1 μ M) revealed sharp reductions in putrescine (undetectable) and spermidine levels (87% decrease vs control) and a 67% increase in spermine levels (lane 7). These results are consistent with the effect of other PTIs on intracellular polyamine levels.²³

Second, an unexpected result was that the DFMO+Spd control (Figure 5: lane 4, 103% relative growth, where the untreated control is set to 100%) had similar intracellular polyamine levels as the combination of **6b**+Spd+DFMO (lane 7, 70% relative growth) and DFMO-only control (lane 2, 64% relative growth). Closer examination revealed that the primary difference between these experiments was the measured intracellular spermidine levels (Figure 5). As intracellular polyamine levels decreased, decreasing intracellular Spd/Spm ratios were observed. Spermidine is important for growth and provides a means to maintain cellular spermine content via biosynthesis (Figure 2).³¹ L3.6pl cells were observed to have normal growth when the Spd/Spm ratio ranged from 2.86 to 0.37. Our data suggest, however, that when the Spd/Spm ratio and Put+Spd+Spm levels drop below a critical threshold, cell growth is reduced. These observations are consistent with other published accounts where critical levels of polyamines must be maintained for proper cell function and growth.^{4a,31}

In short, the reductions observed in both cell growth and intracellular polyamine levels when **6b** is dosed in combination with DFMO+ Spd are all consistent with **6b** acting as an effective PTI. The low K_i value of **6b** (55 nM) observed in competition experiments with 3H -Spd also support this conclusion.

A summary of the design comparisons of the aryl-polyamine series 6–8 is illustrated in Figure 6. First, introduction of terminal *N*-methyl groups was found to decrease the sensitivity of the compound to amine oxidases, without significant loss of its potency as a PTI. In terms of PTI performance, compound **6a** (Trimer44) had consistent potency in both the CHO (EC_{50}

value = 0.34 μM) and L3.6pl (EC₅₀ value = 0.77 μM) cell lines. The *N*-methyl derivative **6b** also displayed similar potency in CHO (EC₅₀ value = 0.42 μM) and L3.6pl cells (EC₅₀ = 1.4 μM). While the potencies were similar, the performance of these two compounds in the absence of aminoguanidine was different. It is important to note that all of the spermidine rescue experiments were performed in the presence of aminoguanidine (AG), a known inhibitor of copper-dependent oxidases which cause the terminal deamination of polyamines.³² Indeed, AG was required to maintain the stability of both spermidine and the polyamine-based PTI under evaluation because compounds containing free-terminal primary amines were potential substrates for amine oxidases in the fetal bovine serum used for cell culture.³³

One method of evaluating the sensitivity of polyamine-based compounds to amine oxidases is to evaluate their innate toxicity in the presence and absence of AG. If the compound is not a substrate for amine oxidases, then it should retain its structure and IC₅₀ value in the presence and absence of a nontoxic dose of AG.³³ The L3.6pl IC₅₀ values of **6a** and **6b** in the presence of AG (250 μM) were 102.8 (± 4.4) and 179.0 (± 11.7) μM , respectively. The L3.6pl IC₅₀ values of **6a** and **6b** in the absence of AG (250 μM) were 188.3 (± 7.6) and 183.4 (± 10.5) μM , respectively. These data support the contention that the *N*-methyl derivative **6b** retained its potency, whereas for **6a**, a good fraction of its activity was lost over the 48 h incubation period. These findings were consistent with observations made with other *N*-methyl polyamine derivatives.³³ In this regard, **6b** provided an alternative design with decreased sensitivity to amine oxidases and with similar potency as **6a**. Future studies are needed, however, to determine if this property provides the intended advantage in vivo. Indeed, decreased sensitivity to amine oxidases could be critical because in vivo experiments are performed without AG present.

Second, a comparison of **6a** and **7b** provided insight into the role of the tether connecting the homospermidine motif to the aryl ring core. Because **7b** contains an amide link, the nitrogen closest to the ring does not bear a formal positive charge at physiological pH. In this regard, **7b** represents an extended version of **6a**, where the homospermidine messages (Figure 6) are presented further away from the aryl core due to the six atom linker in **7b** (i.e., CONH(CH₂)₄). This modification from short tether to longer tether introduced significant toxicity (L3.6pl IC₅₀ of **7b** = 9.7 μM), which resulted in a dramatically lower IC₁₀ value for **7b** (1 μM) and poor PTI properties compared to **6a**. In summary, short tethers provided less toxic PTIs with greater potency.

Third, a comparison of **7a**, **7b**, and **7c** revealed that **7a** was significantly less toxic than **7b** and **7c**, which resulted in IC₁₀ values in L3.6pl cells of >100, 1, and 8 μM for **7a–c**, respectively (Table 2). As shown in Table 2, the high toxicities observed with **7b** and **7c** (as well as **8a** and **8b**) precluded them from being effective PTI agents. While **7a** could act as a PTI, its CHO and L3.6pl EC₅₀ values were 60 and 89.8 μM , respectively. These values were significantly higher than the EC₅₀ values obtained with **6a** and **6b**, indicating that at least in these cell-based assays **7a** had lower potency. We speculate that this was due to the shorter polyamine message (putrescine) displayed by **7a** versus the homospermidine message presented by **6a** and **6b** (Figure 6).

In direct comparisons of putrescine and homospermidine in L1210 cells, the K_m of putrescine was significantly higher than that of homospermidine, indicating a lower affinity for the

PTS.^{2d} Indeed, it is well established that affinity increases across the polyamine series: diamines < triamines < tetraamines.^{2d} This insight could also be applied to **6a** and **7a**. Even though both systems have six atoms separating the aryl core from the second nitrogen of the polyamine chain [i.e., **6a**: CH₂NH-(CH₂)₄ vs **7a**: CONH(CH₂)₄], the presence of the charged nitrogen closest to the ring in **6a** presented a higher affinity homospermidine motif instead of the putrescine message presented by amide **7a** (Figure 6). This is consistent with both the significantly lower K_i value observed with **6a** (Table 2) and the extensive SAR studies by our group with other aryl-polyamine systems.^{13a}

CONCLUSIONS

These studies indicated that a platform which displayed three homospermidine messages provided the most potent PTI of the series evaluated. The triamides (**7b** and **7c**), meta-substituted analogues (**8a** and **8b**), and the para-substituted **5a** system had significant toxicity in the cell lines examined which limited their application as PTIs. The third polyamine arm was shown to be a key part of the PTI design and gave rise to promising compounds (**6a** and **6b**), which efficiently blocked the import of spermidine (1 μM) into DFMO-treated cells as well as the import of ³H-spermidine into untreated cells. PTI **6b** when dosed with DFMO and Spd produced dramatic reductions in intracellular polyamine levels vs the untreated control as well as a 30% reduction in L3.6pl growth after 48 h incubation.

Ultimately, compound **6a** proved to be an excellent PTI with high potency as evidenced by its submicromolar EC₅₀ values in both cell lines evaluated in vitro. The fact that the *N*-methyl analogue **6b** was shown to have decreased sensitivity to amine oxidases and lower toxicity than **6a** provided a new compound with desirable properties for in vivo evaluations. A recent patent has also demonstrated inhibition of putrescine uptake by **6a** in DFMO-treated L3.6pl cells as well as colon cancer (SW620) and other pancreatic cancer cell lines (MiaPaca-2).²⁶ Additional experiments with **6a** also demonstrated its efficacy in combination with DFMO in the presence of exogenous putrescine or spermine in L3.6pl cells (see Supporting Information). Future experiments will test whether these in vitro trends with **6a** and **6b** translate to the appropriate in vivo models.⁶

Lastly, the development of PTIs provides unique tools to examine biological processes dependent upon polyamine transport. For example, the triamide PTI **7a**, which showed modest potency in blocking Spd uptake in this report, was recently shown to be an efficient inhibitor of putrescine uptake in bacteria.³⁴ Specifically, **7a** was used to understand the interplay between the putrescine uptake transporter PlaP and the swarming behavior of *Proteus mirabilis*, a Gram-negative bacterium known to cause urinary tract infections in humans.³⁴ In this regard, compounds with PTI properties may find novel applications in both mammalian and bacterial systems.

EXPERIMENTAL SECTION

Materials. Silica gel 32–63 μm and chemical reagents were purchased from commercial sources and used without further purification. All solvents were distilled prior to use. All reactions were carried out under an N₂ atmosphere. ¹H and ¹³C spectra were recorded at 400 and 75 MHz, respectively. TLC solvent systems were listed as volume percents, and NH₄OH referred to concentrated aqueous ammonium hydroxide. All tested compounds provided

satisfactory elemental analyses as proof of purity ($\geq 95\%$). These are provided in the Supporting Information.

Biological Studies. CHO, CHO-MG*, and L3.6pl cells were grown in RPMI 1640 medium supplemented with 10% fetal bovine serum (FBS) and 1% penicillin/streptomycin. Note: the media must contain L-proline (2 $\mu\text{g}/\text{mL}$) for proper growth of the CHO-MG* cells. All cells were grown at 37 °C under a humidified 5% CO₂ atmosphere. Aminoguanidine (1 mM for CHO and CHO-MG*, and 250 μM for L3.6pl) was added to the growth medium to prevent oxidation of the compounds by the enzyme (bovine serum amine oxidase) present in calf serum. Cells in early to mid log phase were used.

IC₅₀ Determinations. Cell growth was assayed in sterile 96-well microtiter plates (Costar 3599, Corning, NY). CHO and CHO-MG* cells were plated at 10 000 cells/mL. L3.6pl cells were plated at 5000 cells/mL. Drug solutions (10 μL per well) of appropriate concentration in phosphate-buffered saline (PBS) were added after an overnight incubation for each CHO cell line (90 μL of cell suspension used). After exposure to the drug for 48 h, cell growth was determined by measuring formazan formation from the 3-(4,5-dimethylthiazol-2-yl)-5-(3-carboxymethoxyphenyl)-2-(4-sulphenyl)-2H-tetrazolium, inner salt (MTS) using a SynergyMx Biotek microplate reader for absorbance (490 nm) measurements.³⁵ All experiments were run in triplicate.

HPLC and Polyamine Level Determination.³⁶ Briefly, L3.6pl cells (450 000 cells/6 mL media) were incubated with aminoguanidine (250 μM) at 37 °C for 24 h, each compound was added either alone or in combination with other agents as indicated in Figure 5, and the cells were incubated for another 48 h at 37 °C. The cells were then washed with PBS and lysed using a 0.2 M perchloric acid/1 M NaCl solution (200 μL), sonicated, and centrifuged, and the resultant supernatant and pellet were separated. The standard 1,7-diaminoheptane (30 μL of 1.5×10^{-4} M) was added to the polyamine-containing supernatant (100 μL) and then treated at 65 °C for 1 h with 1 M Na₂CO₃ (200 μL) and 18.5 mM dansyl chloride (400 μL) to generate the respective N-dansylated polyamines. Proline (1 M, 100 μL) was added, and the reaction mixture was shaken on a rotary shaker for 20 min at 65 °C. The dansylated products were then extracted into chloroform (2 mL), the organic layer was separated and concentrated, the residue was redissolved in MeOH (1 mL), and each polyamine was then quantified via HPLC analysis.³⁶ The protein content of the pellet was quantified using the Pierce BCA Protein assay kit from Thermo Scientific. Final results are expressed as nmol polyamine/mg protein. Investigation into the media used for these experiments (which contained 10% FBS) revealed a total of 2.6 nmol of putrescine, no detectable spermidine, and 1.6 nmol of spermine that were present in the 6 mL of media used for the experiments. In this regard, minimal exogenous polyamines were available to the growing L3.6pl cells in the nonspermidine-spiked experiments.

K_i Determinations. The inhibition constant for selected PTIs were determined following the protocol of Weeks et al.²³ Briefly, L3.6 pl cells (100 K/well) were seeded into a 24-well plate for log phase growth and incubated with 5% CO₂ for 24 h at 37 °C. The media was then changed with preheated Hanks Balanced Salt Solution (HBSS, containing Ca²⁺ and Mg²⁺) at 37 °C. ³H-Spd (Perkin-Elmer Inc., Boston, MA, fixed at 1 μM) was added with the respective PTI at different PTI concentrations (0, 0.1, 0.3, 1, 2, 3 μM). Cells were incubated at 37 °C for 15 min. The cells were then washed with cold HBSS and lysed with 0.1% sodium dodecyl sulfate (SDS) in water (500 μL). Each cell lysate was then transferred to an Eppendorf tube and centrifuged at 15 000 rpm for 15 min. A sample of each supernatant (200 μL) was transferred into a scintillation vial containing 2 mL of Scintiverse BD, and the resulting scintillation counts were measured. The amount of protein was determined using the Pierce BCA protein assay kit from the remaining lysate volume (approximately 300 μL) to normalize the radioactive counts obtained (pmol ³H-Spd/ μg protein). K_i and K_m values were determined using double reciprocal Lineweaver-Burk plots. The K_i value was determined from the equation $K_i = \text{IC}_{50}/(1 + (L + K_m))$, where IC₅₀ is the concentration of PTI required to block 50% of the relative uptake of

³H-Spd and L is the concentration of ³H-Spd used in the assay (1 μM). The K_m for Spd (666 nM) was calculated by using solutions of ³H-Spd ranging in concentration from 0.3 to 3 μM and plotting the inverse of [³H-Spd] versus the inverse of the pmol Spd/ μg protein/min. The K_m = -1/x intercept.

(S)-2,6-Diamino-N-(3-((4-((3-aminopropyl)amino)butyl)amino)propyl)hexanamide (1b, L-Lys-Spm). Compound 1b was synthesized by a modified method of Weeks et al.²³ ¹H NMR (D₂O) δ 3.92 (t, 1H), 3.38 (m, 1H), 3.27 (m, 1H), 3.12 (m, 10H), 2.91 (t, 2H), 2.18 (m, 2H), 1.89 (m, 4H), 1.77 (m, 4H), 1.71 (m, 2H), 1.39 (m, 2H); matched literature values.^{15,23} HRMS (FAB) *m/z* calcd for C₁₆H₄₃Cl₅N₆O (M + H)⁺ 331.3180, found 331.3175. Anal. C₁₆H₄₃Cl₅N₆O·H₂O, CHN.

N¹,N^{1'},N^{1''}-(Benzene-1,3,5-triyltris(methylene))tris(N⁴-(4-aminobutyl)butane-1,4-diamine) (6a). The N-H Boc-protected compound 20a (0.3948 g, 0.331 mmol) was dissolved in absolute ethanol (10 mL) and stirred at 0 °C for 10 min. A 4 N HCl solution (20 mL) was added to the reaction mixture and stirred overnight. The solution was concentrated, giving the respective amine HCl salt 6a (0.216 g, 71%). ¹H NMR (D₂O, 400 MHz): δ 7.69 (s, 3H, aromatic), 4.35 (s, 6H, CH₂), 3.20 (t, 6H, CH₂), 3.06 (m, 18H, CH₂), 1.79 (m, 24H, CH₂). ¹³C NMR (D₂O): δ 187.9, 135.7, 135.2, 53.2, 49.8, 49.7, 41.7, 26.8, 25.7, 25.6. Matched the literature spectrum, as 6a was synthesized previously.^{13b} Anal. C₃₃H₇₈N₉Cl₉·0.2H₂O, CHN

N¹,N^{1'},N^{1''}-(Benzene-1,3,5-triyltris(methylene))tris(N⁴-(4-methylamino)butyl)butane-1,4-diamine) (6b). The N-Me Boc-protected compound 20b (0.23 g, 0.17 mmol) dissolved in absolute ethanol (10 mL) was stirred at 0 °C for 10 min. A 4 N HCl solution (20 mL) was added to the reaction mixture and stirred overnight. The solution was concentrated, giving the respective amine HCl salt 6b (0.151 g, 85%). ¹H NMR (D₂O, 400 MHz): δ 7.69 (s, 3H, aromatic), 4.35 (s, 6H, CH₂), 3.20 (t, 6H, CH₂), 3.06 (m, 18H, CH₂), 2.74 (s, 9H, CH₃), 1.80 (m, 24H, CH₂). ¹³C NMR (D₂O): δ 135.7, 135.2, 53.2, 51.1, 49.73, 49.69, 35.6, 25.7, 25.5. HRMS (FAB) *m/z* calcd for C₃₆H₇₆N₉ (M + H)⁺ 634.6218, found 634.6197. Anal. C₃₆H₈₄N₉·1.1H₂O, CHN.

N¹,N³,N⁵-Tris(4-((4-aminobutyl)amino)butyl)benzene-1,3,5-tricarboxamide (7a). A solution of Boc-protected 11a (910 mg, 0.67 mmol) was dissolved in absolute ethanol (70 mL) and stirred at 0 °C for 10 min. A 4 M HCl solution (40 mL, 160 mmol) was added to the reaction mixture dropwise and stirred at 0 °C for 30 min and then at room temperature overnight. The solution was concentrated in vacuo to give 7a as a white solid (625 mg, 99%); ¹H NMR (D₂O) δ 8.28 (s, 3H), 3.45 (t, 6H), 3.14 (q, 12H), 3.07 (t, 6H), 1.78 (m, 24H); ¹³C NMR (D₂O) δ 172.0, 138.0, 131.8, 50.3, 49.9, 42.4, 41.8, 28.6, 27.0, 26.1, 25.8. HRMS (FAB) *m/z* calcd for C₃₃H₆₃N₉O₃ (M + H)⁺ 634.5053, found 634.5129. Anal. C₃₃H₆₉Cl₆N₉O₃·3.5H₂O: CHN

N¹,N³,N⁵-Tris(4-((4-((4-aminobutyl)amino)butyl)amino)butyl)benzene-1,3,5-tricarboxamide Nonahydrochloride (7b). A method similar to that described above for 7a was used to make 7b using Boc-protected amine 11b. Light pink solid, 84%. ¹H NMR (D₂O) δ 8.29 (s, 3H), 3.46 (t, 6H), 3.15 (24H), 3.05 (t, 6H), 1.79 (m, 36H); ¹³C NMR (D₂O) δ 171.8, 137.8, 131.9, 50.6, 49.6, 42.4, 41.5, 27.1, 28.8, 27.1, 26.8, 25.8. HRMS (FAB) *m/z* calcd for C₄₅H₉₁N₁₂O₃ (M + H)⁺ 847.7337, found 847.7332. Anal. C₄₅H₉₉Cl₉N₁₂O₃·6H₂O, CHN

N¹,N³,N⁵-Tris(3-((4-((3-aminopropyl)amino)butyl)amino)propyl)benzene-1,3,5-tricarboxamide Nonahydrochloride (7c). The respective solution of the Boc-protected compound 11c (0.40 g, 0.24 mmol), dissolved in absolute ethanol (25 mL), was stirred at 0 °C for 10 min. A 4 N HCl solution (15 mL, 60 mmol) was added dropwise to the reaction mixture and stirred at 0 °C for 20 min and then at room temperature overnight. The solution was concentrated in vacuo to give the respective amine HCl salt as a solid 7c (0.21 g, 80% yield). ¹H NMR (D₂O): δ 8.35 (s, 3H, aromatic), 3.56 (t, 6H, CH₂), 3.23–3.08 (m, 30H, CH₂), 2.17–2.02 (m 12H), 1.89–1.75 (br s, 12H). ¹³C NMR (D₂O): δ 172.1, 137.6, 132.0, 50.0, 49.9, 48.3, 47.5, 39.9, 39.5, 28.6, 26.7, 25.8, 25.7. Anal. C₃₉H₈₇N₁₂O₃Cl₉·3.44H₂O, CHN.

***N*¹,*N*^{1'}-(1,3-Phenylenebis(methylene))bis(*N*⁴-(4-aminobutyl)-butane-1,4-diamine) (8a).** Compound 15a (174 mg, 0.21 mmol) was dissolved in EtOH (30 mL) and stirred at 0 °C for 10 min, and then a 4 M HCl solution (12 mL, 48 mmol) was then added dropwise and stirred for 30 min. The temperature was then allowed to rise to room temperature, and the solution was then stirred under N₂ for 4 h. The solvents were then removed in vacuo to give 8a as a white solid (80 mg, 95% yield). ¹H NMR (D₂O) δ 7.57 (s, 3H), 7.55 (s, 1H), 4.26 (s, 4H), 3.20–3.01 (m, 16H), 1.76 (m, 16H); ¹³C NMR (D₂O) δ 134.7, 133.9, 133.8, 133.0, 53.6, 49.8, 49.5, 41.7, 26.8, 25.7. HRMS (FAB) *m/z* calcd for C₂₄H₄₈N₆ (M + H)⁺ 421.3940, found 421.4013. Anal. C₂₄H₅₄Cl₆N₆·0.6H₂O, CHN.

***N*¹,*N*^{1'}-(1,3-Phenylenebis(methylene))bis(*N*⁴-(4-(4-aminobutyl)amino)butyl)butane-1,4-diamine) (8b).** Compound 15b (130 mg, 0.11 mmol) was dissolved in EtOH (10 mL) and stirred at 0 °C for 10 min, and a 4 M HCl solution (6 mL, 24 mmol) was added dropwise and stirred for 30 min. The temperature was then allowed to rise to room temperature, and the solution was stirred under N₂ for 4 h. The solvents were then removed in vacuo to give a white solid (95 mg, 98%). ¹H NMR (D₂O) δ 7.59–7.57 (m, 4H), 4.30 (s, 4H), 3.17–3.04 (m, 24H), 1.79–1.77 (m, 24H); ¹³C NMR 187.9, 134.4, 133.8, 133.7, 132.9, 53.4, 49.6, 49.3, 41.5, 26.6, 25.5. HRMS (FAB) *m/z* calcd for C₃₂H₆₆N₈ (M + H)⁺ 563.5410, found 563.5483. Anal. C₃₂H₇₄Cl₈N₈·2.5H₂O, CHN.

Polyamines 10a, 10b, and 10c have all been previously synthesized and characterized.^{16,17b,37}

***tert*-Butyl (3-Aminopropyl)(4-((*tert*-butoxycarbonyl)(3-((*tert*-butoxycarbonyl)amino)propyl)amino)butyl)carbamate (Tri-boc-Spermine 10c).** As shown in Scheme 2, spermine free base (1.0 g: 5.1 mmol) was dissolved in 25% MeOH/CH₂Cl₂ solution (200 mL) and stirred at rt, and 2-hydroxybenzaldehyde (0.63 g: 5.1 mmol) was added dropwise. Anhydrous Na₂SO₄ (5.7 g: 40.2 mmol) was added, and the reaction was stirred overnight at rt. ¹H NMR (CDCl₃) showed complete conversion to 12 after overnight stirring at rt. Imine 12 was then consumed in the next step without purification. 12: ¹H NMR (CDCl₃): δ 8.35 (br s, 1H, CH), 7.35–7.19 (br s, 1H, aromatic), 6.99–6.91 (br s, 1H aromatic), 6.90–6.81 (br s, 1H, aromatic), 3.66 (br s, 2H, CH₂), 2.80–2.56 (m, 10H, CH₂). The reaction mixture of 12 was cooled to 0 °C, and di-*tert*-butyl dicarbonate (3.4 g, 15.6 mmol) was added as a solid. The reaction was then stirred for 1.5 h at rt. Upon completion, the volatiles were removed under reduced pressure to provide the tri-Boc imine 13, which was immediately consumed in the next step without purification. 13: ¹H (CDCl₃): δ 8.35 (s, 1H, CH), 3.59 (m, 2H, CH₂), 3.36–3.04 (m, 10H, CH₂). The imine 13 was cleaved using CH₃ONH₂ (1.60 g, 18.7 mmol) and Na₂CO₃ (2.0 g, 18.7 mmol). (Note: Na₂CO₃ was slightly insoluble in MeOH). The reaction turned a cloudy white and then was stirred for 2 h. The volatiles were removed under reduced pressure and redissolved in CH₂Cl₂ (50 mL). The organic layer was washed with aq Na₂CO₃ (~10 wt %), and the organic layer was separated, filtered, and concentrated (4.0 g). Column chromatography (75% CH₂Cl₂/25% hexane) was used to elute the oxime (*R*_f = 0.4) away from the desired product, which remained on the column. The solvent system was then changed to 1% ammonium hydroxide/5% methanol in dichloromethane to elute the product from the column (*R*_f = 0.3). The product, 10c was a sticky oily liquid (1.14 g, 45%). ¹H NMR (CDCl₃): δ: 7.27 (s, 1H, NH), 3.37–3.05 (m, 10H, CH₂) 1.80–1.36 (m, 38H).

[4-(3,5-Bis(4-((*tert*-butoxycarbonyl)-(4-*tert*-butoxycarbonylaminobutyl)amino)butyl)carbonyl)benzoylamino)butyl]-(4-*tert*-butoxycarbonylaminobutyl)-carbamic Acid *tert*-Butyl Ester (11a). A solution of Boc-protected amine 10a¹⁶ (1.80 g, 5.01 mmol) and CH₂Cl₂ (12 mL) was prepared. A solution of K₂CO₃ (1.65 g, 11.94 mmol) and water (20 mL) was added to the original mixture. The tetraalkylammonium phase transfer catalyst Aliquat (0.10 mL) was added and the mixture was cooled to 0 °C. 1,3,5-Benzenetricarboxylic acid chloride 9 (400 mg, 1.51 mmol) in CH₂Cl₂ (24 mL) was added dropwise to the original mixture, allowed to gradually warm, and stirred vigorously at room temperature for 6 h. After the reaction was complete (by ¹H NMR), the solvents were

removed in vacuo, and the residue was redissolved in CH₂Cl₂. The organic layer was then washed with 0.1 M HCl (24 mL), followed by deionized H₂O (24 mL) and saturated aq Na₂CO₃ (24 mL). The organic layer was then separated, dried over anhydrous Na₂SO₄, filtered, and concentrated to give a crude solid which was then purified by flash column chromatography to afford 11a (1.05 g, 56%) as a white solid (*R*_f = 0.25; 4% MeOH/96% CH₂Cl₂); ¹H NMR (CDCl₃) δ 8.41 (s, 3H), 4.75 (br s, 3H), 3.49 (m, 6H), 3.23–3.06 (m, 18H), 2.78–1.30 (m, 78H); ¹³C NMR (CDCl₃) δ 166.5, 156.1, 155.7, 135.2, 128.5, 79.3, 78.9, 46.6, 40.1, 39.8, 28.4, 27.3, 26.4. HRMS (FAB) *m/z* calcd for C₆₃H₁₁₁N₉O₁₅ (M + Na)⁺ 1256.8092, found 1256.8105. Anal. C₆₃H₁₁₁N₉O₁₅·H₂O, CHN.

[4-(3,5-Bis(4-((*tert*-butoxycarbonyl)-(4-*tert*-butoxycarbonyl)-(4-*tert*-butoxycarbonylaminobutyl)amino)butyl)carbonyl)benzoylamino)butyl]-(4-*tert*-butoxycarbonylaminobutyl)-carbamic Acid *tert*-Butyl Ester (11b). A similar procedure was used for 11b, except that Boc-protected polyamine 10b¹⁶ was used. White solid, 75%. ¹H NMR (CDCl₃) δ 8.19 (s, 3H), 3.42 (t, 6H), 3.17 (t, 30H), 1.71–1.41 (m, 117H); ¹³C NMR (CDCl₃) δ 166.4, 156.2, 155.7, 135.4, 128.9, 79.5, 46.8, 45.8, 41.2, 40.5, 39.5, 29.1, 28.5, 27.6, 26.5. Anal. C₉₀H₁₆₂N₁₂O₂₁, CHN.

Boc-Protected Triamide 11c. Tri-Boc spermine 10c (2.27 mmol, 1.14 g) was dissolved in CH₂Cl₂ (10 mL), and a solution of K₂CO₃ (2.27 mmol, 0.313 g) and water (6 mL) was added. Aliquat (1 drop), a phase transfer catalyst, was added, and the mixture was stirred and cooled to 0 °C. A solution of acid chloride 9 (0.69 mmol, 0.183 g) in CH₂Cl₂ (10 mL) was added to the original mixture and after the addition was complete was allowed to warm to rt. The reaction was stirred vigorously overnight. After the reaction was complete, the organic layer was washed with water (20 mL), separated, dried over anhydrous Na₂SO₄, filtered, and concentrated. Column chromatography (95% CH₂Cl₂/5% MeOH) was performed (*R*_f = 0.3). A second column (80% ethyl acetate/20% CHCl₃) was used to remove any remaining impurities (*R*_f = 0.23). The final product was the oil 11c (0.45 g, 40% yield). ¹H NMR (CDCl₃) δ 8.45 (br s, 3H), 7.93 (br s, 1.7H), 7.26 (br s, 0.46H), 5.48 (br s, 1.9H), 5.07 (br s, 0.9H), 3.51–3.0 (m, 42H), 1.93–1.35 (m, 117H); ¹³C NMR (125 MHz, CDCl₃) δ 165.9, 156.5, 156.0, 155.5, 135.5, 128.3, 79.9, 79.6, 78.9, 46.8, 46.2, 44.3, 43.9, 37.5, 36.5, 29.0, 28.6, 28.5, 28.3, 27.7, 26.1. Note: both the ¹H and ¹³C NMR spectra gave rise to broad signals which were expected for this compound type in CDCl₃. Anal. C₈₄H₁₅₀N₁₂O₂₁·0.9H₂O, CHN.

Di-*tert*-butyl ((1,3-Phenylenebis(methylene))bis(azanediy))bis(butane-4,1-diyl)bis(4-((*tert*-butoxycarbonyl)amino)butyl)-carbamate (15a). To maximize the yield, MeOH was dried and distilled prior to this reaction. A solution of 1,3-benzene dicarboxaldehyde 14 (50.0 mg, 0.37 mmol) in 25% MeOH/CH₂Cl₂ (10 mL) was added to a stirred solution of Boc-protected amine 10a (453 mg, 1.26 mmol) in 25% MeOH/CH₂Cl₂ (15 mL). The reaction was then stirred at room temperature under N₂ overnight. After imine formation was complete (by ¹H NMR), the solvents were removed in vacuo and the residue was redissolved in 50% MeOH/CH₂Cl₂ (20 mL). The solution was then cooled to 0 °C followed by addition of predried NaBH₄ (85.3 mg, 2.26 mmol) in small portions, and the mixture was stirred at room temperature under N₂ for 2 h. The volatiles were then removed under reduced pressure, and the residue was redissolved in CH₂Cl₂ and washed three times with aqueous Na₂CO₃. The organic layer was separated, dried over Na₂SO₄, filtered, and concentrated. Column chromatography (*R*_f = 0.25, 25% hexanes/0.1% NH₄OH/74.9% distilled THF) provided compound 15a as a yellow oil (150 mg, 47%). ¹H NMR (CDCl₃) δ 7.28–7.19 (m, 4H), 3.77 (s, 4H), 3.14 (t, 12H), 2.65 (t, 4H), 1.55–1.42 (m, 52H); ¹³C NMR (CDCl₃) δ 156.0, 155.6, 140.5, 128.5, 127.9, 126.7, 79.2, 79.1, 54.0, 49.3, 47.0, 46.9, 46.7, 46.5, 40.2, 28.5, 28.4, 28.3, 27.4, 26.6, 26.1, 26.0, 25.6. HRMS for C₄₄H₈₁N₆O₈ (M + H) calcd: 821.6110; found: 821.6103, Anal. C₄₄H₈₀N₆O₈·0.12H₂O, CHN.

Di-*tert*-butyl ((1,3-Phenylenebis(methylene))bis(azanediy))bis(butane-4,1-diyl)bis(4-((*tert*-butoxycarbonyl)(4-((*tert*-butoxycarbonyl)amino)butyl)amino)butyl)carbamate (15b). To a stirred solution of Boc-protected amine 10b (705 mg, 1.33

mmol) in 25% MeOH/CH₂Cl₂ (20 mL) was added a solution of 1,3-benzene dicarboxaldehyde **14** (52.3 mg, 0.39 mmol) in 25% MeOH/CH₂Cl₂ (15 mL). The reaction was then stirred at room temperature under N₂ overnight. After imine formation was complete by ¹H NMR, the solvents were removed in vacuo, and the residue was redissolved in 50% MeOH/CH₂Cl₂ (25 mL). The solution was then cooled to 0 °C followed by addition of NaBH₄ (88.5 mg, 2.34 mmol) in small portions, and the mixture was stirred at room temperature under N₂ for 2 h. The solvents were then removed under reduced pressure, and the residue was redissolved in CH₂Cl₂ and washed three times with aqueous Na₂CO₃. The organic layer was separated, dried over Na₂SO₄, filtered, and concentrated in vacuo. Column chromatography (R_f = 0.31 (10% MeOH/1% NH₄OH/89% CH₂Cl₂)) provided compound **15b** as a colorless oil (240 mg, 53%). ¹H NMR (CDCl₃) δ 7.32–7.19 (m, 4H), 3.77 (s, 4H), 3.15 (t, 20H), 2.65 (t, 4H), 1.60–1.44 (m, 78H); ¹³C NMR (CDCl₃) δ 156.0, 155.5, 140.5, 128.4, 127.8, 126.7, 79.1, 54.0, 49.3, 46.9, 46.6, 40.2, 28.5, 27.4, 26.1. HRMS (FAB) *m/z* calcd for C₆₂H₁₁₄N₈O₁₂ (M + H)⁺ 1163.8629, found 1163.8629. Anal. C₆₂H₁₁₄N₈O₁₂, CHN.

Benzene-1,3,5-triyltrimethanol (17). Trimethyl 1,3,5-benzene-tricarboxylate **16** (5 g, 0.02 mmol) in dry THF (75 mL) was added through a pressure-equalized addition funnel into a 500 mL round-bottom flask containing LiAlH₄ (3.8 g, 100 mmol) at 0 °C. The mixture was allowed to warm to room temperature and stirred overnight (14 h). The reaction was quenched by the slow addition of a 1:1 mixture of Celite and NaHSO₄. The suspension was filtered, and Celite was washed with EtOH (100 mL). The solvent was removed under reduced pressure, and the crude triol **17** was obtained (4.71 g). This crude solid was consumed in the next step without further purification. ¹H NMR (DMSO): δ 7.12 (s, 3H, aromatic), 5.12 (br s, 3H, CH₂), 4.47 (s, 6H, OH), which matched its literature spectrum.^{13b}

Benzene-1,3,5-tricarbaldehyde (18). The crude triol **17** (1 g, 5.9 mmol) was dissolved in 150 mL of *tert*-butyl alcohol. 2-Iodoxybenzoic acid (IBX, 9.83g, 47.2 mmol) was added to the triol mixture, and the reaction was stirred and heated to reflux in an oil bath at 95 °C for 2 h. The reaction was monitored by TLC (35% EtOAc/65% hexane, R_f = 0.39). The mixture was concentrated, resuspended in 35% EtOAc/65% hexane, and filtered to remove the bulk of the IBX byproduct. The filtrate was concentrated, dissolved in CH₂Cl₂, and washed with 10% aqueous Na₂CO₃. The organic layer was separated, dried with anhydrous Na₂SO₄, filtered, and concentrated in vacuo. Column chromatography (3% EtOH/97% CHCl₃, R_f = 0.39) was performed and provided the product **18** (0.75g, 79%). ¹H NMR (CDCl₃): δ 10.21 (s, 3H, CHO), 8.64 (s, 3H, aromatic), which matched the literature spectrum.²⁰ Note: aldehyde **18** is also commercially available from the Sigma-Aldrich Company.

***tert*-Butyl (4-((4-Aminobutyl)(*tert*-butoxycarbonyl)amino)butyl)(methyl)carbamate 19.** This compound was previously reported by our group.^{17b}

Tri-*tert*-butyl (((((Benzene-1,3,5-triyltris(methylene))tris(azanediyl))tris(butane-4,1-diyl))tris(*tert*-butoxycarbonyl)azanediyl))tris(butane-4,1-diyl)tricarbamate 20a. This compound was synthesized previously.^{13b} Briefly, Boc-protected homospemidine **10a** (0.72 g, 2 mmol) was dissolved with 25% MeOH/CH₂Cl₂. 1,3,5-Triformylbenzene **18** (0.10 g, 0.63 mmol) was added to the mixture and stirred for 3 h under a N₂ atmosphere. Loss of the aldehyde CH signal at δ 10.21 was confirmed by ¹H NMR (CDCl₃). The solvent was then removed under reduced pressure, and the crude material was redissolved in 50% MeOH/CH₂Cl₂. To this new solution was added NaBH₄ (0.24 g, 6.3 mmol) at 0 °C, and the reaction was stirred overnight at rt under a N₂ atmosphere. Loss of the imine was confirmed by ¹H NMR. The solvent was then removed under reduced pressure. A base workup was performed by redissolving the residue in CH₂Cl₂ and washing with aqueous Na₂CO₃. The organic layer was separated, dried over anhydrous Na₂SO₄, filtered, and concentrated to give a yellow oil (1.13 g). Column chromatography (30% MeOH/69% acetonitrile/1% NH₄OH) was used to reisolate the unreacted amine starting material (R_f = 0.7) and provide the trisubstituted aryl compound **20a** (0.35 g, 47%).^{13b} ¹H NMR (CDCl₃): δ 7.14 (s, 3H, aromatic), 4.69 (s, 3H, NH), 3.75 (s, 6H, CH₂), 3.15 (br s, 18H,

CH₂), 2.65 (t, 6H, CH₂), 1.61–1.5 (m, 78H, CH₂, CH₃). ¹³C NMR (D₂O) δ 172.0, 138.0, 131.8, 50.3, 49.9, 42.4, 41.8, 28.6, 27.0, 26.1, 25.8.^{13b}

Tri-*tert*-butyl (((((Benzene-1,3,5-triyltris(methylene))tris(azanediyl))tris(butane-4,1-diyl))tris(*tert*-butoxycarbonyl)azanediyl))tris(butane-4,1-diyl)tricarbamate 20b. *N*-Methylamine derivative **19** (0.72 g, 1.94 mmol) was dissolved in 25% MeOH/CH₂Cl₂ (10 mL) and 1,3,5-triformylbenzene **18** (0.081 g, 0.50 mmol) was added. The reaction mixture was stirred overnight under a N₂ atmosphere. Loss of the starting material was monitored by loss of the aldehyde CH (δ 10.21) in the ¹H NMR. Upon the conversion of the starting material, the solvent was removed by concentrating the sample on a rotary evaporator. The crude material was redissolved in a solution of 50% MeOH/CH₂Cl₂. To this new solution, NaBH₄ (0.18 g, 4.77 mmol) was added at 0 °C and the reaction was stirred overnight at rt under a N₂ atmosphere. Loss of the intermediate imine was monitored by ¹H NMR. The solvent was removed under reduced pressure. A base workup was performed by redissolving the residue in CH₂Cl₂ and washing the organic layer with aqueous Na₂CO₃. The organic layer was separated, dried over anhydrous Na₂SO₄, filtered, and concentrated to give a crude oil (0.73 g). Column chromatography (5% MeOH in CH₃CN containing 1% NH₄OH) was used to reisolate the unreacted amine starting material (R_f = 0.65). The column was then flushed with (50% MeOH in CH₃CN containing 1% NH₄OH) to provide the pure trisubstituted aryl compound **20b** (0.32 g, 39%). ¹H NMR (CDCl₃, 400 MHz): δ 7.15 (s, 3H, aromatic), 3.76 (s, 6H, CH₂), 3.48 (m, 3H, NH), 3.19 (m, 18H CH₂), 2.83 (s, 9H, CH₃), 2.65 (t, 6H, CH₂), 1.75–1.40 (m, 78H CH₂, CH₃). ¹³C NMR (CDCl₃, 100 MHz): 155.8, 155.6, 140.1, 126.7, 79.2, 54.0, 49.4, 48.7, 48.1, 46.9, 34.1, 28.5, 27.4, 26.6, 26.1, 25.3. HRMS (FAB) *m/z* calcd for C₆₆H₁₂₄N₉O₁₂ (M + H)⁺ =1234.9364, found 1234.9355. C₆₆H₁₂₃N₉O₁₂·0.8 H₂O, CHN.

■ ASSOCIATED CONTENT

Supporting Information

¹H spectra for known compound **1b**, ¹H and ¹³C NMR spectra for compounds **6b**, **7a–c**, **8a**, **8b**, **11a–c**, **15a**, **15b**, and **20b**; elemental analyses for **1b**, **6a**, **6b**, **7a–c**, **8a**, **8b**, **11**, **15**, and **20b**, and titration experiments with **6a** in L3.6pl cells in the presence of a fixed dose of DFMO and exogenous putrescine (or spermine). This material is available free of charge via the Internet at <http://pubs.acs.org>.

■ AUTHOR INFORMATION

Corresponding Author

*Phone: (407) 823-6545. E-mail: Otto.Phanstiel@ucf.edu.

Notes

The authors declare no competing financial interest.

■ ACKNOWLEDGMENTS

The authors thank the 2011 Department of Defense Congressionally Directed Medical Research Program (CDMRP) Peer Review Cancer Research Program (PRCRP) Discovery Award CA110724 for financial support of this research and Dr. Isaiah Fidler at the University of Texas M. D. Anderson Cancer Center for the generous gift of L3.6pl cells for this research.

■ ABBREVIATIONS USED

PTI, polyamine transport inhibitor; DFMO, α -difluoromethylornithine; PTS, polyamine transport system; DFMO+PTI, α -difluoromethylornithine used in combination with a polyamine transport inhibitor; DFMO+Spd, α -difluoromethylornithine used in combination with spermidine; DFMO+Spd+PTI, α -difluoromethylornithine used in combination with spermidine and a polyamine transport inhibitor; ODC, ornithine decarboxylase; L-Lys-Spm, L-lysine spermine conjugate (used

in this study); D-Lys-Spm = MQT 1426, D-lysine spermine conjugate (not used in the study); SCC, squamous cell carcinoma; PSV, polyamine sequestering vesicles; CHO, Chinese hamster ovary; CHO-MG, Chinese hamster ovary cells which are defective in polyamine transport; CHO-MG*, Chinese hamster ovary cells which are defective in polyamine transport and were derived from CHO-MG; AG, amino-guanidine; Spd, spermidine; SOX, spermine oxidase; PAO, polyamine oxidase; SSAT, spermidine-spermine acetyl transferase; IC₁₀ value, the highest concentration of compound which resulted in ≤10% cell growth inhibition (i.e., ≥90% cell viability) vs an untreated control over the same time period; IC₅₀ value, the concentration of compound which resulted in 50% cell growth inhibition vs an untreated control over the same time period; HBSS, Hank's balanced salt solution; SDS, sodium dodecyl sulfate

REFERENCES

- (1) (a) Cullis, P. M.; Green, R. E.; Merson-Davies, L.; Travis, N. Probing the mechanism of transport and compartmentalization of polyamines in mammalian cells. *Chem. Biol.* **1999**, *6*, 717–729. (b) Seiler, N.; Delcros, J.-G.; Moulinoux, J. P. Polyamine transport in mammalian cells. An update. *Int. J. Biochem.* **1996**, *28*, 843–861. (c) Seiler, N.; Dezeure, F. Polyamine transport in mammalian cells. *Int. J. Biochem.* **1990**, *22*, 211–218. (d) Casero, R. A.; Marton, L. J. Targeting polyamine metabolism and function in cancer and other hyperproliferative diseases. *Nat. Rev. Drug Discovery* **2007**, *6*, 373–390. (e) Coffino, P. Regulation of cellular polyamines by antizyme. *Nat. Rev. Mol. Cell Biol.* **2001**, *2* (3), 188–194.
- (2) (a) Phanstiel, O.; Price, H. L.; Wang, L.; Juusola, J.; Kline, M.; Shah, S. M. The effect of polyamine homology on the transport and cytotoxicity properties of polyamine–(DNA intercalator) conjugates. *J. Org. Chem.* **2000**, *65*, 5590–5599. (b) Wang, L.; Price, H. L.; Juusola, J.; Kline, M.; Phanstiel, O., IV. Influence of polyamine architecture on the transport and topoisomerase II inhibitory properties of polyamine DNA–intercalator conjugates. *J. Med. Chem.* **2001**, *44*, 3682–3691. (c) Wang, C.; Delcros, J.-G.; Biggerstaff, J.; Phanstiel, O. Synthesis and biological evaluation of N1-(anthracen-9-ylmethyl)triamines as molecular recognition elements for the polyamine transporter. *J. Med. Chem.* **2003**, *46*, 2663–2671. (d) Wang, C.; Delcros, J.-G.; Biggerstaff, J.; Phanstiel, O. Molecular requirements for targeting the polyamine transport system: Synthesis and biological evaluation of polyamine anthracene conjugates. *J. Med. Chem.* **2003**, *46*, 2672–2682. (e) Wang, C.; Delcros, J.-G.; Cannon, L.; Konate, F.; Carias, H.; Biggerstaff, J.; Gardner, R. A.; Phanstiel, O. Defining the molecular requirements for the selective delivery of polyamine conjugates into cells containing active polyamine transporters. *J. Med. Chem.* **2003**, *46*, 5129–5138. (f) Kaur, N.; Delcros, J.-G.; Martin, B.; Phanstiel, O. Synthesis and biological evaluation of dihydromotuporamine derivatives in cells containing active polyamine transporters. *J. Med. Chem.* **2005**, *48*, 3832–3839. (g) Gardner, R. A.; Delcros, J.-G.; Konate, F.; Breitbeil, F.; Martin, B.; Sigman, M.; Phanstiel, O. N1-Substituent effects in the selective delivery of polyamine-conjugates into cells containing active polyamine transporters. *J. Med. Chem.* **2004**, *47*, 6055–6069. (h) Barret, J. M.; Kruczynski, A.; Vispe, S.; Annereau, J. P.; Brel, V.; Guminski, Y.; Delcros, J. G.; Lansiaux, A.; Guilbaud, N.; Imbert, T.; Bailly, C. F14512, a potent antitumor agent targeting topoisomerase II vectored into cancer cells via the polyamine transport system. *Cancer Res.* **2008**, *68* (23), 9845–9853. (i) Kruczynski, A.; Pillon, A.; Creancier, L.; Vandenberghe, I.; Gomes, B.; Brel, V.; Fournier, E.; Annereau, J. P.; Currie, E.; Guminski, Y.; Bonnet, D.; Bailly, C.; Guilbaud, N. F14512, a polyamine-vectorized anti-cancer drug, currently in clinical trials exhibits a marked preclinical anti-leukemic activity. *Leukemia* **2013**, 1–10.
- (3) Wallick, C. J. G. L.; Thorne, M.; Feith, D. J.; Takasaki, K. Y.; Wilson, S. M.; Seki, J. A.; Pegg, A. E.; Byus, C. V.; Bachmann, A. S. Key role for p27Kip1, retinoblastoma protein Rb, and MYCN in polyamine inhibitor-induced G1 cell cycle arrest in MYCN-amplified human neuroblastoma cells. *Oncogene* **2005**, *24*, 5606–5618.
- (4) (a) Meyskens, F. L., Jr.; Gerner, E. W. Development of Difluoromethylornithine (DFMO) as a chemoprevention agent. *Clin. Cancer Res.* **1999**, *5*, 945–951. (b) Fabian, C. J.; Kimler, B. F.; Brady, D. A.; Mayo, M. S.; Chang, C. H.; Ferraro, J. A.; Zalles, C. M.; Stanton, A. L.; Masood, S.; Grizzle, W. E.; Boyd, N. F.; Arneson, D. W.; Johnson, K. A. A Phase II breast cancer chemoprevention trial of oral alpha-difluoromethylornithine: Breast tissue, imaging, and serum and urine biomarkers. *Clin. Cancer Res.* **2002**, *8*, 3105–3117. (c) Abeloff, M. D.; Slavik, M.; Luk, G. D.; Griffin, C. A.; Hermann, J.; Blanc, O.; Sjoerdsma, A.; Baylin, S. B. Phase I trial and pharmacokinetic studies of alpha-difluoromethylornithine—an inhibitor of polyamine biosynthesis. *J. Clin. Oncol.* **1984**, *2*, 124–130.
- (5) Ask, A.; Persson, L.; Heby, O. Increased survival of L1210 leukemic mice by prevention of the utilization of extracellular polyamines. Studies using a polyamine-uptake mutant, antibiotics and a polyamine-deficient diet. *Cancer Lett.* **1992**, *66* (1), 29–34.
- (6) Chen, Y.; Weeks, R. S.; Burns, M. R.; Boorman, D. W.; Klein-Szanto, A. Combination therapy with 2-difluoromethylornithine and a polyamine transport inhibitor against murine squamous cell carcinoma. *Int. J. Cancer* **2006**, *118*, 2344–2349.
- (7) Burns, M. R.; Graminski, G. F.; Weeks, R. S.; Chen, Y.; O'Brien, T. G. Lipophilic lysine-spermine conjugates are potent polyamine transport inhibitors for use in combination with a polyamine biosynthesis inhibitor. *J. Med. Chem.* **2009**, *52*, 1983–1993.
- (8) Skorupskil, K. A.; O'Brien, T. G.; Guerrero, T.; Rodriguez, C. O.; Burns, M. R. Phase I/II clinical trials of 2-difluoromethylornithine (DFMO) and a novel polyamine transport inhibitor (MQT 1426) for feline oral squamous cell carcinoma. *Vet. Comp. Oncol.* **2011**, *9*, 275–282.
- (9) (a) Igarashi, K.; Kashiwagi, K. Polyamine transport in bacteria and yeast. *Biochem. J.* **1999**, *344*, 633–642. (b) Heinick, A.; Urban, K.; Roth, S.; Spies, D.; Nunes, F.; Phanstiel, O., IV; Liebau, E.; Luersen, K. *Caenorhabditis elegans* P_{5B}-type CATP-5 operates in polyamine transport and is crucial for norspermidine-mediated suppression of RNA interference. *FASEB J.* **2010**, *24*, 206–217. (c) de Tezanos Pinto, F.; Corradi, G. R.; de la Hera, D. P.; Adamo, H. P. CHO cells expressing the human P(5)-ATPase ATP13A2 are more sensitive to the toxic effects of herbicide paraquat. *Neurochem. Int.* **2012**, *60* (3), 243–248. (d) Sala-Rabanal, M.; Li, D. C.; Dake, G. R.; Kurata, H. T.; Inyushin, M.; Skatchkov, S. N.; Nichols, C. G. Polyamine transport by the polyspecific organic cation transporters OCT1, OCT2, and OCT3. *Mol. Pharm.* **2013**, *10* (4), 1450–1458. (e) Aouida, M.; Poulin, R.; Ramotar, D. The human carnitine transporter SLC22A16 mediates high affinity uptake of the anticancer polyamine analog bleomycin-A5. *J. Biol. Chem.* **2010**, *285* (9), 6275–6284. (f) Uemura, T.; Stringer, D. E.; Blohm-Mangone, K. A.; Gerner, E. W. Polyamine transport is mediated by both endocytic and solute carrier transport mechanisms in the gastrointestinal tract. *Am. J. Physiol.: Gastrointest. Liver Physiol.* **2010**, *299* (2), G517–G522. (g) Poulin, R.; Casero, R. A.; Soulet, D. Recent advances in the molecular biology of metazoan polyamine transport. *Amino Acids* **2012**, *42*, 711–723.
- (10) (a) Soulet, D. C. L.; Kaouass, M.; Charest-Gaudreault, R.; Audette, M.; Poulin, R. Role of endocytosis in the internalization of spermidine-C(2)-BODIPY, a highly fluorescent probe of polyamine transport. *Biochem. J.* **2002**, *367*, 347–357. (b) Soulet, D.; Gagnon, B.; Rivest, S.; Audette, M.; Poulin, R. A fluorescent probe of polyamine transport accumulates into intracellular acidic vesicles via a two-step mechanism. *J. Biol. Chem.* **2004**, *279*, 49355–49366.
- (11) (a) Belting, M.; Persson, S.; Fransson, L.-A. Proteoglycan involvement in polyamine uptake. *Biochem. J.* **1999**, *338*, 317–323. (b) Belting, M.; Mani, K.; Jonsson, M.; Cheng, F.; Sandgren, S.; Jonsson, S.; Ding, K.; Delcros, J.-G.; Fransson, L.-A. Glypican-1 is a vehicle for polyamine uptake in mammalian cells: A pivotal role for nitrosothiol-derived nitric oxide. *J. Biol. Chem.* **2003**, *278*, 47181–47189.
- (12) Bergeron, R. J.; McManis, J. S.; Weimar, W. R.; Schreier, K.; Gao, F.; Wu, Q.; Ortiz-Ocasio, J.; Luchetta, G.; Porter, C.; Vinson, J.

R. The role of charge in polyamine analogue recognition. *J. Med. Chem.* **1995**, *38*, 2278–2285.

(13) (a) Phanstiel, O., IV; Kaur, N.; Delcros, J.-G. Structure-activity investigations of polyamine-anthracene conjugates and their uptake via the polyamine transporter. *Amino Acids* **2007**, *33*, 305–313. (b) Kaur, N.; Delcros, J.-G.; Imran, J.; Khaled, A.; Chehtane, M.; Tschammer, N.; Martin, B.; Phanstiel, O., IV. A comparison of chloroambucil- and xylene-containing polyamines leads to improved ligands for accessing the polyamine transport system. *J. Med. Chem.* **2008**, *51*, 1393–1401.

(14) Phanstiel, O.; Archer, J. J. Design of polyamine transport inhibitors as therapeutics. In *Polyamine Drug Discovery*, 1st ed.; Casero, R. W. P., Ed.; Royal Society of Chemistry: London, 2011; p 302.

(15) Burns, M. R.; Carlson, C. L.; Vanderwerf, S. M.; Ziemer, J. R.; Weeks, R. S.; Cai, F.; Webb, H. K.; Graminski, G. F. Amino acid/spermine conjugates: Polyamine amides as potent spermidine uptake inhibitors. *J. Med. Chem.* **2001**, *44*, 3632–3644.

(16) Gardner, R. A.; Kinkade, R.; Wang, C.; Phanstiel, O., IV. Total synthesis of petrobactin and its homologues as potential growth stimuli for *Marinobacter hydrocarbonclasticus*, an oil-degrading bacteria. *J. Org. Chem.* **2004**, *69*, 3530–3537.

(17) (a) Kaur, N.; Delcros, J.-G.; Archer, J.; Weagraff, N. Z.; Martin, B.; Phanstiel, O., IV. Designing the polyamine pharmacophore: Influence of N-substituents on the transport behavior of polyamine conjugates. *J. Med. Chem.* **2008**, *51*, 2551–2560. (b) Muth, A.; Kamel, J.; Kaur, N.; Shicora, A. C.; Ayene, I. S.; Gilmour, S. K.; Phanstiel, O., IV. Development of Polyamine Transport Ligands with Improved Metabolic Stability and Selectivity against Specific Human Cancers. *J. Med. Chem.* **2013**, *56*, 5819–5828.

(18) Khomutov, A. R.; Shvetsov, A. S.; Vepsalainen, J. J.; Kritzyn, A. M. Novel acid-free cleavage of *N*-(2-hydroxyarylidene) protected amines. *Tetrahedron Lett.* **2001**, *42*, 2887–2889.

(19) Corce, V.; Morin, E.; Guiheneuf, S.; Renault, E.; Renaud, S.; Cannie, I.; Tripier, R.; Lima, L. M.; Julienne, K.; Gouin, S. G.; Loreal, O.; Deniaud, D.; Gaboriau, F. Polyaminoquinoline iron chelators for vectorization of antiproliferative agents: Design, synthesis, and validation. *Bioconjugate Chem.* **2012**, *23* (9), 1952–1968.

(20) Van Arman, S. A. 2-Methyl-2-propanol as a solvent for *o*-iodobenzoic acid (IBX) oxidation of 1° alcohols to aldehydes. *Tetrahedron Lett.* **2009**, *50*, 4693–4695.

(21) Delcros, J.-G.; Tomasi, S.; Carrington, S.; Martin, B.; Renault, J.; Blagbrough, I. S.; Uriac, P. Effect of spermine conjugation on the cytotoxicity and cellular transport of acridine. *J. Med. Chem.* **2002**, *45*, 5098–5111.

(22) (a) Mandel, J. L.; Flintoff, W. F. Isolation of mutant mammalian cells altered in polyamine transport. *J. Cell. Physiol.* **1978**, *97*, 335–344. (b) Byers, T. L.; Wechter, R.; Nuttall, M. E.; Pegg, A. E. Expression of a human gene for polyamine transport in chinese hamster ovary cells. *Biochem. J.* **1989**, *263*, 745–752.

(23) Weeks, R. S.; Vanderwerf, S. M.; Carlson, C. L.; Burns, M. R.; O'Day, C. L.; Cai, F.; Devens, B. H.; Webb, H. K. Novel lysine-spermine conjugate inhibits polyamine transport and inhibits cell growth when given with DFMO. *Exp. Cell Res.* **2000**, *261*, 293–302.

(24) Heaton, M. A.; Flintoff, W. F. Methylglyoxal-bis-(guanyldrazone)-Resistant Chinese Hamster Ovary Cells: Genetic Evidence That More Than A Single Locus Controls Uptake. *J. Cell. Physiol.* **1988**, *136*, 133–139.

(25) Frydman, B. J.; Marton, L. J.; Reddy, V. K.; Valasinas, A. L.; Witiak, D. T. Conformationally Restricted Polyamines. U.S. Patent 5,889,061, March 30, 1999.

(26) Phanstiel, O.; Archer, J. J. Polyamine Transport Inhibitors as Novel Therapeutics. WO 2010/148390 A2, 2010.

(27) American Cancer Society. *Cancer Facts & Figures 2013*; American Cancer Society: Atlanta, 2013; p 25.

(28) Bruns, C. J.; Harbison, M. T.; Kuniyasu, H.; Eue, I.; Fidler, I. J. In vivo selection and characterization of metastatic variants from human pancreatic adenocarcinoma by using orthotopic implantation in nude mice. *Neoplasia* **1999**, *1* (1), 50–62.

(29) (a) Basuroy, U. K.; Gerner, E. W. Emerging concepts in targeting the polyamine metabolic pathway in epithelial cancer

chemoprevention and chemotherapy. *J. Biochem.* **2006**, *139*, 27–33. (b) Azmi, A. S.; Ahmad, A.; Banerjee, S.; Rangnekar, V. M.; Mohammad, R. M.; Sarkar, F. H. Chemoprevention of pancreatic cancer: Characterization of Par-4 and its modulation by 3,3'-diindolylmethane (DIM). *Pharm. Res.* **2008**, *25*, 2117–2124.

(30) Grossie, V. B., Jr.; Ota, D. M.; Ajani, J. A.; Nishioka, K. Effect of intravenous alpha-difluoromethylornithine on the polyamine levels of normal tissue and a transplantable fibrosarcoma. *Cancer Res.* **1987**, *47* (7), 1836–1840.

(31) Casero, R. A., Jr.; Marton, L. J. Targeting polyamine metabolism and function in cancer and other hyperproliferative diseases. *Nat. Rev. Drug Discovery* **2007**, *6* (5), 373–390.

(32) (a) Nilsson, B. O.; Kockum, I.; Rosengren, E. Inhibition of diamine oxidase promotes uptake of putrescine from rat small intestine. *Inflammation Res.* **1996**, *45* (10), 513–518. (b) Holttä, E.; Pulkkinen, P.; Elfving, K.; Janne, J. Oxidation of polyamines by diamine oxidase from human seminal plasma. *Biochem. J.* **1975**, *145* (2), 373–378. (c) Gahl, W. A.; Pitot, H. C. Reversal by aminoguanidine of the inhibition of proliferation of human fibroblasts by spermidine and spermine. *Chem.-Biol. Interact.* **1978**, *22* (1), 91–98. (d) Morgan, D. M. Polyamine oxidases and oxidized polyamines. In *Physiology of Polyamines*; Bachrach, U.; Heimer, Y. M., Eds.; CRC Press: Boca Raton, FL, 1989; Vol. 1, pp 203–229.

(33) Bergeron, R. J.; Feng, Y.; Weimar, W. R.; McManis, J. S.; Dimova, H.; Porter, C.; Raisler, B.; Phanstiel, O. A comparison of structure-activity relationships between spermidine and spermine analogue antineoplastics. *J. Med. Chem.* **1997**, *40*, 1475–1494.

(34) Kurihara, S.; Sakai, Y.; Suzuki, H.; Muth, A.; Phanstiel, O., IV; Rather, P. N. Putrescine importer PlaP contributes to swarming motility and urothelial cell invasion in *Proteus mirabilis*. *J. Biol. Chem.* **2013**, *288* (22), 15668–15676.

(35) Mosmann, T. Rapid colorimetric assay for cellular growth and survival: Application to proliferation and cytotoxic assays. *J. Immunol. Methods* **1983**, *65*, 55–63.

(36) Minocha, S. C.; Minocha, R.; Robie, C. A. High-performance liquid chromatographic method for the determination of dansyl-polyamines. *J. Chromatogr.* **1990**, *511*, 177–183.

(37) (a) Gardner, R. A.; Belting, M.; Svensson, K.; Phanstiel, O., IV. Synthesis and transfection efficiencies of new lipophilic polyamines. *J. Med. Chem.* **2007**, *50*, 308–318. (b) Geall, A. J.; Blagbrough, I. S. Homologation of polyamines in the synthesis of lipo-spermine conjugates and related lipoplexes. *Tetrahedron Lett.* **1998**, *39*, 443–446.